HIGH IMPEDANCE FAULT IDENTIFICATION AND LOCALIZATION IN MV DISTRIBUTION FEEDERS

P. T. De Silva

(128859X)

Degree of Master of Science in Electrical Engineering

Department of Electrical Engineering

University of Moratuwa

Sri Lanka

June 2017

HIGH IMPEDANCE FAULT IDENTIFICATION & LOCALIZATION IN MV DISTRIBUTION FEEDERS

P. T. De Silva

(128859X)

Dissertation submitted in partial fulfillment of the requirements for the

Degree Master of Science in Electrical Engineering

Department of Electrical Engineering

University of Moratuwa

Sri Lanka

June 2017

DECLARATION OF THE CANDIDATE & SUPERVISOR

I declare that this is my own work and this dissertation does not incorporate without acknowledgement any material previously submitted for a Degree or Diploma in any other University or institute of higher learning and to the best of my knowledge and belief it does not contain any material previously published or written by another person except where the acknowledgement is made in the text.

Also, I hereby grant to University of Moratuwa the non-exclusive right to reproduce and distribute my dissertation, in whole or in part in print, electronic or other medium. I retain the right to use this content in whole or part in future works (such as articles or books).

Signature: Date:

The above candidate has carried out research for the Masters Dissertation under our supervision.

Signature of the supervisor: Date
Prof J. R. Lucas

Signature of the supervisor: Date
Dr P. S. N.De Silva

Abstract

High Impedance Faults (HIF) in distribution feeders are kind of an abnormal condition that most of the electric distribution utilities face if they are maintaining a bare overhead distribution network. These faults cause not only poor quality of supply to the consumers but an immense threat to their lives, if not well managed. By nature, identification and localization of these faults are very hard due to the limited current it draws from the source. But the severe potential threat remains same as it takes distribution medium voltage in to human reach unnoticed.

This study focuses on developing a methodology that can be simply implemented by the utilities to identify and localize the HIF. As a summary, starting from data acquisition, this study identifies a methodology to detect and localize the HIF and finally provides an insight on how to implement the proposed methodology.

Data acquisition is one of the main difficulties faced by the distribution utilities to monitor and identify the network conditions and take necessary precautions over the anomalies before or after the particular incidents. This is mainly due to the high cost incurred for each measuring device installed in the field with the required insulation levels up to the operating voltage classes. This study has proposed a unique time stamp based data acquisition device (based on the concept of Phasor Measurement Units) mounted on top of the conductors to collect the required data and wirelessly transmit over to a terminal unit mounted on the pole. The transmitted data is then processed in this pole mounted concentrator and notifies a central server about the identified network anomaly.

Extensive simulation analysis carried out by this study using MATALAB SIMULINK shows that the proposed methodology provides an accurate way to identify and localize the HIF under various network operational conditions.

Acknowledgement

It is my great pleasure to express gratitude to those who were behind me in completing my research project.

Firstly, I would like to express my sincere gratitude to my supervisor Prof. J. R. Lucas for his great insights and perspective with much patience throughout the entire period and Dr. Narendra De Silva for his continuous support with his immense knowledge motivating me to do this research. Their guidance helped me in all the time starting of this research, up until the end and writing of this thesis. Thank you very much for giving me the opportunity to work with you both.

In addition, I would like to thank all the lecturers in Department of Electrical Engineering and Post Graduate Office, Faculty of Engineering, who engaged in this MSc course in various ways to educate us and broaden our vision.

My sincere thanks go to my managers and colleagues at Lanka Electricity Company (Private) Limited who help me in many ways during this period.

Finally, I would be thankful to my family members including my wife, parents, brother and sister who always encourage and help me to complete this research.

Table of Contents

List of Figures

List of Tables

List of Abbreviations

Abbreviation	Description
HIF	High Impedance Faults
KPI	Key Performance Indicators
SAIFI	System Average Interruption Frequency Index
SAIDI	System Average Interruption Duration Index
AI	Artificial Intelligence
PPS	Pulse per Second
DFT	Discrete Fourier Transformation
FFT	Fast Fourier Transformation
PUCSL	Public Utilities Commission of Sri Lanka
kWh	Kilo Watt Hour
IEEE	Institute of Electrical and Electronic Engineers
IEC	International Electrotechnical Commission

CHAPTER1

1. INTRODUCTION

The Power System which supplies electricity to the consumer basically comprises of generation, transmission, and distribution. All these areas are treated equally and developed in parallel to avoid bottle necks in delivering the generated power to the end-consumer. However in a financial and technical sense, it is very common that the distribution sector gets reduced focus, compared to the generation and transmission, in most of the countries. Yet, it is often the most critical component since it directly takes the system power up to consumers in every nook and corner, has the highest power quality issues, has the highest reliability issues and has the highest technical and non-technical losses. This study is focused on such a critical yet less addressed problem in the power distribution sector and proposed a novel, less expensive practical implementation methodology.

1.1. High Impedance Fault

Earth faults occurring in electrical distribution systems can be categorized into two different categories depending on their salient attributes with respect to the fault impedance. The first one is where the fault impedance is below a hundred ohms and the other one is where the fault impedance is in the order of a few hundred or thousands of ohms.

Overhead bare distribution conductors are more prone to physical contact or arc with nearby objects which are mostly not very conductive but quasi insulating objects like vegetation, cement walls, aged insulators and dry ground when fallen to ground once broken [1]. Suresh [2] identifies the faults currents for different common surface with a voltage level of 12.5 kV and results are tabulated in table 1.1.

Table 1.1Faults Current for Different Common Surfaces

Surface	Current (A)
Dry asphalt	0
Concrete (non reinforced)	0
Dry Sand	0
Wet sand	15
Dry grass	25
Wet grass	50
Reinforced concrete	75

The significance of all is that these faults do not draw enough current to operate the conventional over current protection mechanisms, such as fuses and over current relays, if the instruments are not specifically designed. This small fault current, or the very small increment, in the feeders appears to be a normal load increment during the operation [3]. Therefore, these faults are not easy to identify and locate in the midst of the operation. Most of the time, they are beyond the reach of protective relays, zero sequence overvoltage relays or over current relays. They are difficult to detect and even if detected, the situation can be most difficult to discriminate from normal operation. In general, these faults are called as High Impedance Faults (HIF).

1.2. High Impedance Fault Characteristics

Other than the above discussed hardly detectable low currents which exist due to the fact that HIF have high impedance in the fault path, there is another salient phenomenon that occurs with HIF. This is the presence of arcing, which is the main focus of this study to distinguish HIF.

Arcing happens as a result of the air gap breakdown between the conductor and a quasi-insulated object, which is sometimes the earth surface. Due to the gradient difference in the electric field between the conductors and the object, when HIF happens, live conductors create a voltage difference over a short distance [4]. When this voltage accumulates to a specific magnitude in each half-cycle and then the air

gap starts to break down and as a result arcing is produced. The practical waveforms and analysis of HIF are rarely documented due to the fact that practical experiments on system faults are costly. HRL Technology Pvt Ltd [4] provides the data for arcing faults from an 18 day program of ignition testing. Testing has been carried out at 12,700V (the conductor-to-earth voltage of 22kV networks) at realistic fault currents, ranging from 4.2A to 1kA to develop a model to predict the probability of fire ignition from electric arcs in network faults. This study has identified that as the arc current approaches zero, it is slightly distorted from a true sinusoidal waveform due to the influence of arc voltage. This causes the current to flow in the opposite direction within a short period. Because of this reverse current flow, the arc cannot be reestablished immediately. Therefore, after this happens, there is a time gap that no current flows, which is commonly referred to as the 'current zero pause'. This is an influencing factor in the detail distortions around the zero crossing points of the HIF current waveform which creates number of harmonics [4].

As for B. T. Phung [5], randomness and intermittency is another characteristic of HIF, mainly due to the presence of the arcing phenomena. Researchers have observed that the fault current cannot exist in steady state for a long period of time due to sudden variations in the fault current waveform. The arc, which extinguishes or reignites, heavily depends on the open air cooling conditions of the area. Random motion of the contacted or grounded quasi insulated objects, such as trees or conductor, are also not stable paths for fault currents, which make it highly intermittent.

Further Nara [5] identifies that distortion and harmonics are also a salient characteristic of HIF, as the arcing phenomenon and ground path nonlinearity distort the fault current waveform. When the amplitude of the fault current is comparatively small, due to the high impedance, the nonlinearity becomes more obvious and significant, which in turn generates more harmonics in the waveform.

1.3. Significance of High Impedance Fault Detection

Fault identification and localization plays a vital role in the entire distribution system operation. The faster the particular faults are identified and localized, the sooner the power can be restored to the consumers. Sometimes HIF creates an immense burden on system operators and field staff, as it hard to locate. Field staff repetitively switches on and off the load breakers and route their vehicles empirically, to isolate sections to find the exact location of the fault. This process can sometimes take few of hours. Even today, from the author's experience, utilities use traditional over current or conventional earth fault protective devices to detect HIF, by adjusting its values to make it compatible with HIF currents. But this has led in to many unexpected service interruptions caused by non-fault conditions to the consumers, which reduce the reliability key-performance-indices (KPIs) of utilities. In order to get rid of these situations, utilities who are even having dedicated HIF detectors increase the fault current settings to reduce these interruptions. This creates server threat to the human lives as it can ignite fire.

Due to the arcing, HIF can sometimes even create heavy voltage sags and flickering at the consumer side. This may heavily affect the utilities quality performance indicators such and SAIDI and SAIFI and ultimately end up with a poor quality and unreliable supply.

Customer expectations and regulatory requirements also demand improved power quality, reliability, and operational flexibility from distribution utilities. Therefore, electrical utilities are now under increased pressure to clear these kinds of faults as faster as possible and speed up the restoration process to power up the consumers [6].

1.4. Existing HIF Identification and Localizing Methodologies

Identification and localization of earth faults have been one of the main research topics in the field of electricity distribution system protection studies in past few decades, and several methodologies have been investigated varying from simple pole top hardware assemblies to complex artificial neural networks. However, HIF detection is still a challenge for protection and operations engineers. Numerical

relays located at the beginning of each distribution feeder with current and voltage sensors, provide a greater sensitivity, accuracy and selectivity over various fault types including HIFs. However, practical implementations of these advanced methods are somewhat limited due to the incurred cost and other technical restrictions.

1.4.1. Impedance Based Fault Localization Methods

Impedance based fault techniques are very popular in the transmission network protection systems. However, when it comes to the distribution systems, there are some limitations using this technology. Mora-Flòrez [7] discusses the performance of 10 fault location methods for power distribution systems and compared the results. All the 10 methods use only the measurements of voltage and current at the primary substation level. Out of this voltage and current, they estimate the apparent impedance viewed from the substation measurement point. Difference between pre-fault and fault impedance, together with the network parameters are used to estimate the distance to the fault point. One of the drawbacks of this method is, all the uncertainties, such as the estimation of the distance to the fault, caused by the unknown impedance value of fault is treated under different assumptions.

C. Orozco-Henao [8] proposed an analytical methodology based on the minimum fault reactance concept. The core idea of this approach is that, for each analyzed distribution network segment, a random value for the fault distance estimate is supposed. By using this random value and network circuit analysis equations, the fault reactance can be estimated. The assumed fault distance value is then systematically varied, from reference bus to the line length section. For each assumed fault distance, a fault reactance is estimated. This procedure is repeated on all system lines. Considering that most line faults are resistive in nature, the chosen fault location is the one that generates the smaller fault reactance estimate. Then a Fibonacci search approach is proposed as a systematic variation strategy to estimate fault distance.

One of the main aspects related to these analyses is the assumed direct influence of the fault resistance and distance between fault and measurement point. The higher

the fault resistance and distance to the fault, the bigger the estimation error of the system. Therefore, due to the scattered radial nature, with lots of spur lines of the distribution network and importantly with HIF, impedance based fault identification is not revealing the accurate location of the fault [9].

1.4.2. Knowledge Based Fault Localization Methods

With the development and popularization of computer based analysis, knowledge based fault localization has become one of prime focus for detecting distribution system faults, including HIF. Knowledge based fault localization methods can be mainly categorized into three categories and they are, Artificial intelligence and statistical analysis based methods, Distributed device based methods and Hybrid methods [9]. Artificial intelligence (AI) and statistical analysis based methods runs are based on several AI methods like Artificial Neural networks (ANN), Expert Systems, Fuzzy Logic and Genetic Algorithms etc. Martins [10] has proposed a methodology using Eigen values and artificial neural network based learning algorithm. The neural network is trained to map the non-linear relationship existing between fault location and characteristic Eigen values. According to the paper, the main characteristics and particularities of this method are reduced number of input signals, recognition of the fault type and identification of faulty line or lines, location of the fault and independence value. However, the author has not mentioned any specific methodology to identify and locate HIFs.

Wang [11] suggests a mathematical algorithm for detecting fault sections and affected areas on radial distribution networks. To obtain the voltage data, they use scattered voltage sensor network at various locations on the consumer ends. This method uses messages obtained from these voltage sensors and topological information of distribution networks to detect and locate the faults and affected areas. The Algorithm is developed in C++. First they have formed matrix for the relation of the voltage sensors with sections. Then another matrix is constructed based on the topological relation between each section and node in the distribution network. Faulty sections and location can be found using matrix operation as suggested in the paper. This also limits the detection and localization of HIF depending on the voltage

sensor sensitivity. It is not practical to use many voltage sensors in medium voltage network due to the cost incurred for each sensor unit.

Carl [12] describes a commercial product developed by the researchers at Texas A&M University who have licensed this technology to the GE who has developed a commercial device for utility use. Since characteristics of high-impedance faults are widely varying, this paper suggested that it is unrealistic to expect a single algorithm to detect even a majority of faults. So they have used knowledge based multiple detection approaches, with an intelligent relay system capable of simultaneously meeting requirements of a broad range of fault types. This system yields a confidence level related to the probability or assumption that a fault is present or not. With these confidence levels for different algorithms, they conclude the type of fault and whether it is a HIF or not. It requires the current and the spectral content of each current signal. Then it calculates several components from this spectrum and comes to different conclusions depending on the algorithm. As an example, a load pattern analyzer has the task of differentiating situations like a fallen conductor is on the ground or is still on top of the pole, but in contact with some foreign object. Further it can detect failing system operation component like cracked or contaminated insulator which is causing arcs. Author suggests these kind of sensitive decisions also can be made out of this system. However, it is mentioned that all the algorithms do not perform equally well in their detection of a given particular fault. Because different algorithms detect different fault types or sometimes fault combinations, there may be exist some errors or overlapping regions between the algorithm detections which adds complexity to the system decision.

It is identified that these knowledge based fault localization techniques more often rely on external inputs such as substation and feeder circuit breaker status, SCADA systems data, feeder voltage and current sensors and metering data. These complex situations add reliability factors to the decision which reduces the confidence level of the particular decision.

1.4.3. Frequency Components and Traveling Wave Based Methods

The methods based on Frequency Components and Traveling Waves identify and localize the HIF using frequency spectrum and fault generated travelling wave reflections respectively. This is also a long researched area to detect and localize HIFs.

Macedo [13] has proposed a methodology to detect HIFs based on the analysis of the behavior of inter harmonic currents associated with electric arcs. According to the author, the origin of inter harmonic currents is associated with random variations of electric arc during HIF fault conditions. Therefore, the higher the variation and randomness of the HIF faults, the greater will be the inter-harmonic content with the current flow. The proposed solution acquires the data of instantaneous current signals of the feeders from a discrete data acquisition system developed with a microcontroller. It identifies immediately adjacent inter harmonic frequencies to the fundamental frequency and detects the HIFs. A test site having a medium voltage network with several soil types has been built specifically for validating this prototype. Jichao Chen [14] Has developed a new algorithm for HIF detection which is based on the extracted features from the original signal by using the Wavelet Transform method. The detection criterion is developed from a subset of WT coefficients which makes the algorithm relatively simpler and faster to implement. Mohd Syukri Ali [15] has proposed a methodology of identifying the fault location using discrete wavelet transform based Multi Resolution Analysis and a database. This study analyses the three phase voltages at the main substation. The 1st, 2nd and 3rd level of detail wavelet transform coefficients are extracted for each phase and used for the identification of faulty section using a data base. The fault data base has been constructed using simulation results obtained from PSCAD. Once the fault has occurred, the methodology analyses two cycles of the voltage signal and HIF is detected using the detailed surge coefficient with respect to the predefined and constructed values in the database.

Ali-Reza [16] has suggested a new HIF detection quite similar to the method of Mohd Syukri Ali [15] where this also used a combination of wavelet transform and

statistical technique as a fault detection methodology. The Methodology includes the current coefficients of level 1 and 2 decomposed with a software "rbior" as mother wavelet for the feature extraction, and principal component analysis has been used for the feature selection. Finally Bayes classifier has been used as the HIF detection out of the selection. Various HIFs with different surfaces like wet and dry asphalt, cement and soil, and transient states data has been gathered from experimental tests and simulated using Electro Magnetic Transients Program (EMTP). According to the paper the results show a high success rate of this to detect HIF, but since this is a probabilistic approach there is some probability for wrong selection and detection of HIF as well.

1.4.4. Research Study

The current research develops a methodology to detect high impedance faults using the three current phasors of the distribution system. A pre-calibrated conductor mounted "A to D" converter unit acquires the current waveforms by high frequency sampling. The device contains a GSP receiver to get the universal coordinated time (UTC) to synchronize the internal clock with the UTC. It receives the 1 pulse per second PPS from the satellite whose rising edge is aligned to UTC time second boundary. This allows obtaining the sampled data on all three devices, mounted on each phase, to common time reference.

This three, time stamped, data is sent to a pole top mounted remote terminal unit (RTU) using radio frequency communication. A zig-bee mesh network containing four nodes is proposed for physical implementation. The RTU then estimates the residual waveform of the time referenced three current waveforms using a Kalman filter and search for the harmonic currents associated with the HIF. If an anomaly in harmonic content is detected, it sends a fault detection signal to a central server. The central server analyzes the fault location according to a nodal matrix depending on the geographical distribution of fault locators and radial distribution network which scattered geographically. The algorithm is simulated using a model of actual distribution network developed in MATLAB/SIMULINK environment. The results show that proposed methodology can be practically implemented to detect and

localize the HIF faults in the electricity distribution network using an optimization algorithm to spread the minimum number of devices to get the maximum results. Using these devices, utilities can narrow the faulted area but the size of the estimated geographic area depends on the number of deployed devices.

CHAPTER 2

2. PROJECT OVERVIEW

2.1. Scope of the Project

Distribution utilities all over the world face significant power quality and reliability issues incurred due to the HIFs on their distribution networks. Despite being a highly researched area, most of the utilities have been unable to address this issue to improve the system performance due to various restrictions such as implementation investment (cost), commercial availability of technology, lack of proven results, poor performance records, lack of experience. Even the mostly adopted high impedance fault (HIF) detection algorithms are still under research levels and above mentioned issues still holds and preventing them to see the sunlight in implementation.

There are several types of faults in the electricity distribution systems, which can be mainly categorized in to two types, namely symmetrical faults and asymmetrical faults. A Symmetrical fault can be considered as a severe fault because it is drawing high magnitude of current but these faults occur infrequently in the distribution systems. These can be easily detected using traditional fault detecting devices. According to the author's experience as an electrical engineer in the distribution supply industry, approximately two percent of total faults are symmetrical faults in the distribution system. These faults occur as line to line to line to ground (L-L-L-G) and line to line to line (L-L-L) faults. The other type which is asymmetric faults is the most common fault type not only in the distribution network but as a whole power system. There are mainly three types, namely line to ground (L-G), line to line (L-L) and double line to ground (LL-G) faults. Out of these faults L-G faults are the most common faults in the electricity distribution systems which the high impedance line to ground fault are the most hard to detect faults. Therefore this study develops a methodology to detect and localize the L-G high impedance faults using harmonic characteristic of the fault zero-sequence current as per the figure 2.1.

2.2. Data Acquisition Using Current Phasors

In data acquisition systems, it is a must to electrically isolate the measurement points from the system especially in hazardous voltage classes. Generally opto-isolators, pulse transformers and current transformers are used to isolate the low voltage signals. However, it not that easy to isolate the transducers in medium voltage networks which incur a great extent of cost. Cost impact due to the high insulation that needs to maintain over the line to line and line to ground voltage and current transducers, it is very difficult to justify residual current detection based fault locators to scatter around the distribution network to detect ground faults specially the HIFs.

Therefore this study has used a current phasor based conductor mounted analog-to-digital converter which uses its GPS receiver to get the 1 PPS and synch its internal clock to UTC in order to get the sampled data with the universal time stamp.

2.3. Estimation of Residual Current Using Kalman Filtering Approach

Feeder currents are not stationary. Even the rms values are time-varying in nature and contains significant amount of noises due to the dynamics of distribution network loads and faults. Therefore, a Kalman Filter based approach has been used in this research to analyze the residual current of the three phases. Each of above mentioned time-stamped current signals is analyzed at the RTU which is mounted in the near vicinity of these conductor mounted analog-to-digital converters. The RTU combines all three current waveforms in order to construct the residual current waveform and estimates the residual current waveform using a Kalman filter to get rid of the noise associated with the raw signals and digital signal processing.

2.4. Identification of HIF Using Third Harmonics in Estimated Residual Current

As per the S. R. Nam [17] and Naser Zamanan [18], in most of the HIFs, the current third harmonic is generated more than the 50% of the total harmonic distortion. However, this can happen due to the non linear load switching such as capacitor bank switching in the line currents. However, those switching does not appear in the

residual currents, and only zero sequent current associated distortion appears in the residual waveforms. Using this property, HIF is detected and an estimate of the third harmonic level content is sent to the central server which decides the exact location of the fault using a nodal matrix.

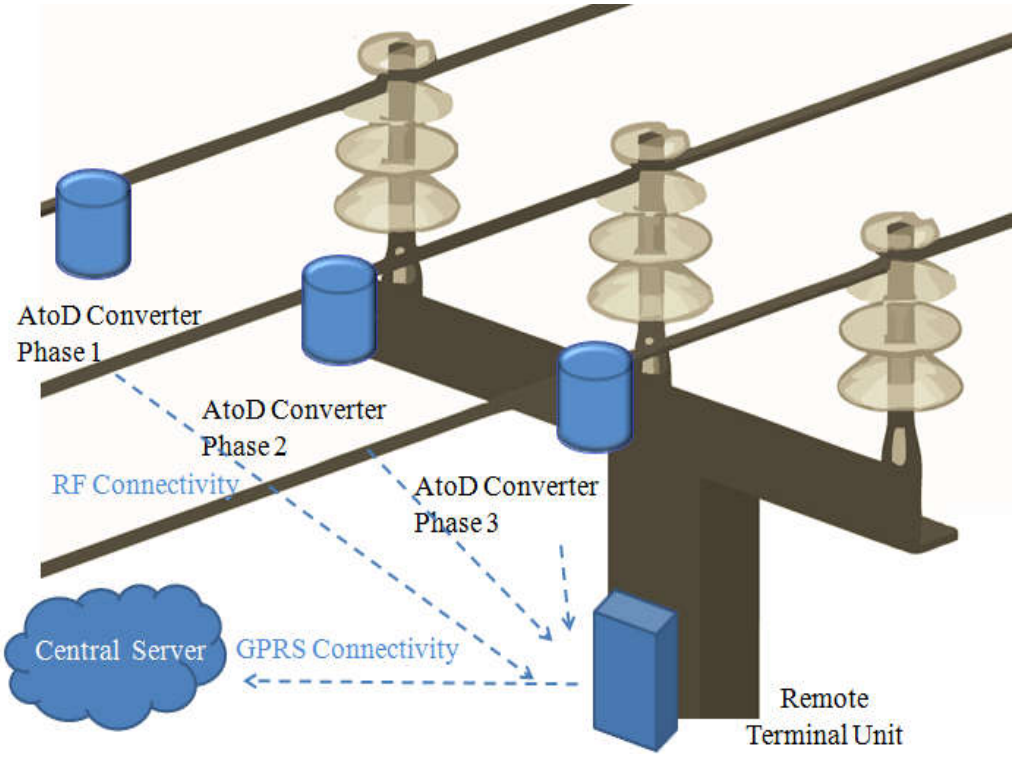

Figure 2.1 Proposed System Overview

CHAPTER 3

3. METHODOLOGY

3.1. Phasor Representation of Current Waveforms

Phase angles of voltage and current phasors of electricity network buses have always been of special interest to electricity power system engineers. From basics of load flow study theorem, it is known that active power flow in a power line is nearly proportional to the sine of the angle difference between voltages at the considering two nodes of the line. However, distribution engineers are rarely using theses phasor properties in their operations as they tend to use root mean square (RMS) values in their day to day general use. RMS magnitudes are said to be sufficient enough for them to work with. However, considering an RMS value only for a voltages and currents, we are missing a considerable amount of information associated with both current and voltage phasor parameters.

An AC waveform can be mathematically be represented in their general symbols as,

$$x(t) = Xm\cos(\omega t + \varphi) \tag{3-1}$$

This is shown in figure 3.1.

In a phasor notation, this waveform is represented with peak values as,

$$X = X_m \angle \phi \tag{3-2}$$

Since RMS quantities are generally used with alternating quantities, the equivalent RMS is obtained by a scale factor of $1/\sqrt{2}$ on the magnitude. Then the synchrophasor is defined as the magnitude and angle of a fundamental frequency waveform as referenced to a cosine signal which is represented as,

$$X = \frac{X_m}{\sqrt{2}} \angle \phi \tag{3-3}$$

This can be represent in complex numbers as follows,

$$X = (Xm/\sqrt{2})\, e\, j\phi = (Xm/\sqrt{2})\, [\cos\phi + j \sin\phi] \quad (3\text{-}4)$$

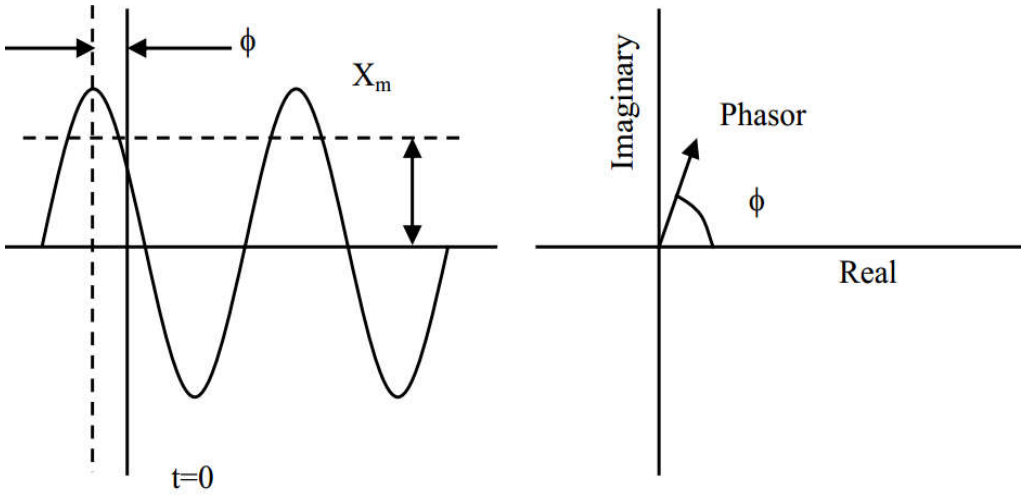

Figure 3.1 Sinusoidal and it's Phasor Representation

3.2. Data Sampling

Assuming that the signal frequency is constant, a time span of 20 cycles is considered in this research for the data window of the phasor estimation. For each cycle of these 20 cycles, 20 phasors are extracted by the Fourier transform which is implemented as the Discrete Fourier transform (DFT) algorithm. For the simplicity of this research, leakage phenomena and off-nominal frequency have not been considered. However, this may have to be included to the digital signal processing algorithms when considered in the practical implementation.

3.2.1. Time Stamp Insertion

Time stamp for each 20 cycles which spans a duration of 400ms is inserted to the array of data. Figure 3.2 shows the time stamps are shown as time reference 1 and 2 which are stamped one per each cycle. Then the duration in between these two and

the duration between two peaks of the cycles are calculated. If the two measurements are different, we have to conclude that there is an error in the measurements which needs to be corrected.

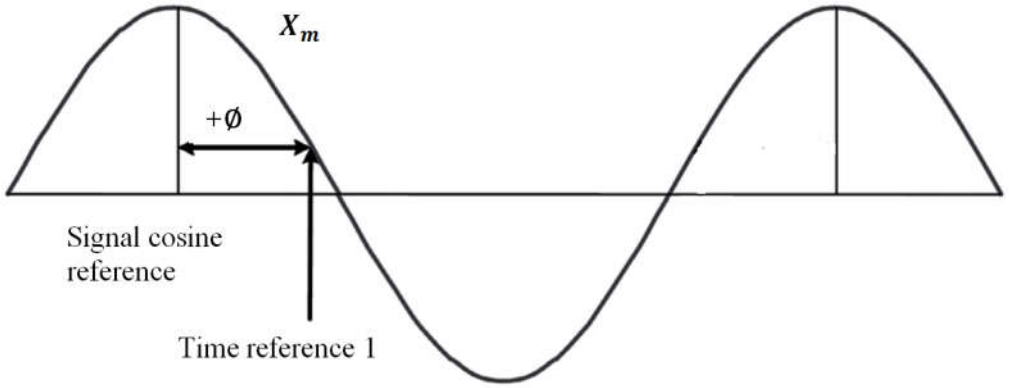

Figure 3.2 Waveform Time Stamp

At the instant that time reference 1 occurs, there is an angle that is shown as + and, magnitude of the waveform of is Xm. Similarly, next time reference also calculated in equal spaces and check for the errors if available. If not this time stamped data is stored and transmitted to the RTU. Internal clock that obtain the time stamp data is synch with the UTC time reference via GPS receiver. Overall data acquisition process is illustrated in figure 3.3.

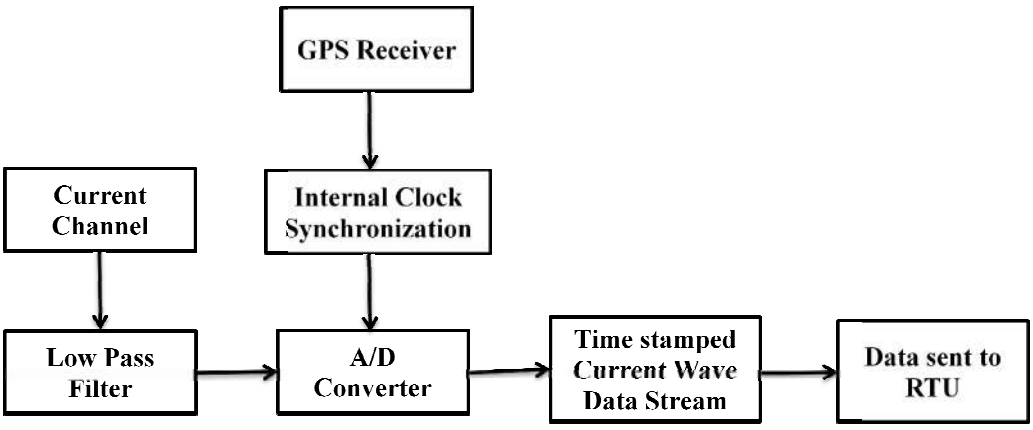

Figure 3.3 Block Diagram of Conductor Mounted Device

3.2.2. Fourier Transform

The Fourier transform decomposes a function or a signal of time domain into its component frequencies. The Fourier transform of a function of time domain is a complex function in the frequency domain, which its absolute value represents the amount of that frequency component present in the original time domain function. The complex or the imaginary part represents the phase offset of the that particular frequency component. In mathematical terms Fourier transform of a x(t) function is given by,

$$X_f = \int_{\infty}^{\infty} x(t) e^{-j2xft} dt \tag{3-5}$$

The inverse Fourier transform can be used to recover the original time function from its Fourier transform.

3.2.3. Discrete Fourier Transform (DFT)

DFT is a method of calculating the Fourier transform of a finite number of samples of a signal taken from a finite, framed input. This is calculated at discrete steps in the frequency domain, just as the input signal is sampled at discrete instants in the time domain.

The computation of phasors of currents starts with samples of the waveform taken at uniform intervals of Δt. This sampled data can be considered as a time function x(t) consisting of uniformly spaced pulses, each with a magnitude x(kΔT).

$$\mathrm{x(t)} = \sum_{\mathrm{k}=-\infty}^{\infty} \mathrm{x(k\Delta T)\ \delta(t \quad k\Delta T)} \tag{3-6}$$

If the cut off frequency of the current signal is greater than one-half of the sampling frequency, the Fourier transform of the sampled data will be different from that of the input signal which can be seen inverse transform is obtained to construct the signal again. This happens due to the phenomenon known as aliasing. Therefore, the Nyquist criteria states that the bandwidth of the input signals must be less than half the sampling frequency utilized in obtaining the sampled data. As the high

frequency components of the current signal are not of much interest for phasor analysis, a sampling frequency of 1.5 kHz has been used, and which can be easily implemented by a micro-controller and which is sufficient to identify the harmonics up to 15^{th} harmonic.

3.2.4. Recursive Waveform Updates

As the phasor calculation is a continuous process, it is necessary to consider algorithms which will update the phasor estimate as newer data samples are acquired in each sampling cycles. When new sample dataset arrives, the period old data set is replaced by the new data set. In this case, if a particular window contains N samples, there will be N-1 common samples with previous calculation for the DFT calculation. That means, the phasor estimate with data from the new window is the same as the phasor estimate with data from the old window when the input signal is a constant sinusoid. However, even the non recursive method is more convenient for use, it can continue an error in the estimate from one window to the entire estimation. Because then, this error is always present in all the phasor estimates from thereafter. Therefore, this negative attribute of the recursive phasor algorithms must be kept in mind when practical implementation of these algorithms. However, because of the great computational efficiency of the recursive algorithm, it has been chosen for the recursive updating as the algorithm in this study.

3.2.5. Residual Waveform Estimation at RTU

All three time referenced signals are then sent to the pole mounted data concentrator or generally called as remote terminal unit (RTU). RTU acquires these three signals from each device and stored in an array for the calculation of residual current waveform.

With the reference obtained, the residual current of three phases is calculated by performing a vector summation and constructed the residual waveform for the 20 cycle period. Then this residual current is estimated through a Kalman filter for the possible third harmonic components to detect HIF which will be elaborated in chapter 4.

3.2.6. Kalman Filter Approach

The Kalman filter is one of important and common real world data representation algorithms in use today. It has been very common and spread in wide variety of applications from simple mathematical simulations to aerospace engineering applications. Since it is recursive, new measurements can be processed as and when they arrive. This property is the main influence to use a Kalman filter in this HIF detection methodology. Since real word current signals are varying rapidly, small fault currents need to be identified in this noisy and rapidly varying environment. If the noise is gaussian, the Kalman filter minimizes the mean square error of the estimated parameters due to the noise.

With the inputs given, Kalman filter keeps track of the estimated state of the system or the function and the variance or uncertainty of the estimate. The previous estimate is updated using a state transition model and measurements from the sensors which will be elaborated in chapter 4. Basic block diagram of the Kalman filter is illustrated in figure 3.4.

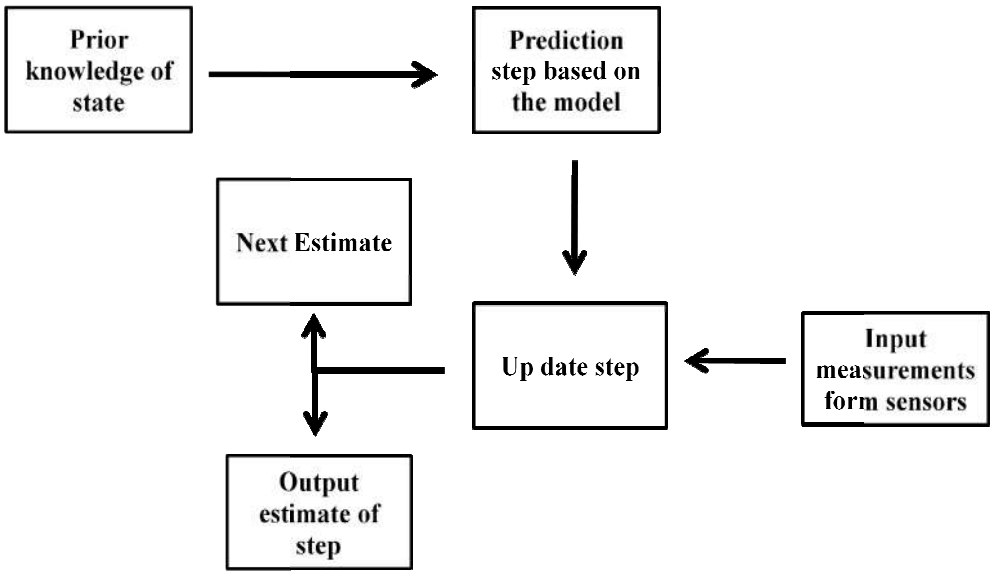

Figure 3.4 Basic Block Diagram of the Kalman Filter

As in the other sensor systems, the waveform samples obtained in the section 3.1.7 contain information, noise, as well as measurement errors of the CTs. Therefore a

filtering technique is required to condition the data before estimating the residual waveform and make decisions. Sometimes variables of a waveform like amplitude, phase angle changes in predictable ways and sometimes random events like faults may cause unexpected changes to these variables. However, the most critical thing is, it may not be sure whether an abrupt or unexpected change in a measurement is caused due to an actual change in the system like load changes and switching operations or is due to noise or a fault. Therefore, Kalman filtering technique based method has been implemented to filter out such noisy scenarios as much possible while responding to the measurements optimally and estimating the state accurately.

3.2.7. Developing the State Space Model of a Current Waveform

In order to apply the Kalman filtering method, it is necessary to build the state space model of the residual current waveform obtained from combining three phase current phasors. Now these current phasors are in complex form model after the Discrete Fourier Transformation. The phasor representation of kth harmonic component is in the state as given in equation 3.7.

$$X_k = \frac{1}{\sqrt{2}}\frac{2}{N}\sum_{n=0}^{N-1} x(n\ \ T)e^{\frac{-j2xkn}{N}} \tag{3-7}$$

Where in trigonometric complex functions, given as in equation 3.8,

$$X_k = \frac{\sqrt{2}}{N}\sum_{n=0}^{N-1} x(n\ \ T)\{\cos\left(\frac{2xkn}{N}\right)\quad j\sin(\frac{2xkn}{N})\} \tag{3-8}$$

by using the general notation x(nΔT) is as the measurement of nth sample and 2π/N=θ where θ is the sampling angle measured in terms of the period of the fundamental frequency component, it is possible to modify the equation to form given in equation 3.9 and 3.10.

$$X_k = \frac{\sqrt{2}}{N}\sum_{n=0}^{N-1} x_n\{\cos(kn\theta)\quad j\sin(kn\theta)\} \tag{3-9}$$

$$X_k = \frac{\sqrt{2}}{N}\sum_{n=0}^{N-1} x_n\{\cos(kn\theta)\} \quad \frac{\sqrt{2}}{N}\sum_{n=0}^{N-1} x_n\{\sin(kn\theta)\} \tag{3-10}$$

In order to develop the state space model of the system, it is necessary to have to develop the state transition matrix for the estimation of residual current phasor at sampling time (n+1)ΔT in terms of residual current phasor at (n) ΔT. If the two states of this waveform are considered as the real and imaginary part of the waveform, the equation 3.11 can be obtained follows.

$$I_k = I_r \quad jI_i \tag{3-11}$$

Then as per the Kalman filter requirements, state equation with these two states can be written as in equation 3.12.

$$\begin{bmatrix} i_{r(n+1)} \\ i_{i(n+1)} \end{bmatrix} = A \begin{bmatrix} i_{r(n)} \\ i_{i(n)} \end{bmatrix} + B \begin{bmatrix} \Delta i_r \\ \Delta i_i \end{bmatrix} \tag{3-12}$$

Where,

[A] is the state transition matrix which advances the phasor by one sampling interval.

[B] is the driving function matrix which advances the changes [Δi(n)] by one sampling interval.

$i_{r(n+1)}$and$i_{i(n+1)}$are the real component and imaginary component of the(n+1)thcurrent phasor.

$i_{r(n)}$and$i_{i(n)}$are the real component and imaginary component of the (n)th current phasor.

Therefore for a sinusoidal wave, state transition matrix [A] and the driving matrix [B] will be the same. [A] is rotating the phasor through an angle that corresponds to one sampling interval. If the sampling time is ΔT, change of the phase angle due to the rotation of the phasor in one sampling interval is (ώΔT). Therefore, the [A] matrix for the model of a single frequency sinusoid is as given in equation 3.13.

$$[A] = [B] = \begin{bmatrix} \cos(\omega \Delta T) & \sin(\omega \Delta T) \\ \sin(\omega \Delta T) & \cos(\omega \Delta T) \end{bmatrix} \tag{3-13}$$

Since we are interested in third harmonic level to identify the HIF, we need at least four state variables to define the state transition matrix to represent the fundamental and third harmonic in-phase and quadrature-phase components. The modified state transition matrix will be as follows.

$$[A] = [B] = \begin{bmatrix} \cos(\omega\ T) & \sin(\omega\ T) & 0 & 0 \\ \sin(\omega\ T) & \cos(\omega\ T) & 0 & 0 \\ 0 & 0 & \cos(3\omega\ T) & \sin(3\omega\ T) \\ 0 & 0 & \sin(3\omega\ T) & \cos(3\omega\ T) \end{bmatrix} \tag{3-14}$$

Once we set up the state transition matrix, the state transition equation is as follows,

$$\begin{bmatrix} i_{r(n+1)} \\ i_{i(n+1)} \end{bmatrix} = \begin{bmatrix} \cos(\acute{\omega}\Delta T) & \sin(\acute{\omega}\Delta T) \\ \sin(\acute{\omega}\Delta T) & \cos(\acute{\omega}\Delta T) \end{bmatrix} \begin{bmatrix} i_{r(n)} \\ i_{i(n)} \end{bmatrix} + \begin{bmatrix} \cos(\acute{\omega}\Delta T) & \sin(\acute{\omega}\Delta T) \\ \sin(\acute{\omega}\Delta T) & \cos(\acute{\omega}\Delta T) \end{bmatrix} \begin{bmatrix} \Delta i_r \\ \Delta i_i \end{bmatrix} \tag{3-15}$$

State transition equation considering the third harmonics is as follows,

$$\begin{bmatrix} i_{r(n+1)} \\ i_{i(n+1)} \\ i_{3r(n+1)} \\ i_{3i(n+1)} \end{bmatrix} = \begin{bmatrix} \cos(\acute{\omega}\Delta T) & \sin(\acute{\omega}\Delta T) & 0 & 0 & i_{r(n)} \\ \sin(\acute{\omega}\Delta T) & \cos(\acute{\omega}\Delta T) & 0 & 0 & i_{i(n)} \\ 0 & 0 & \cos(3\acute{\omega}\Delta T) & \sin(3\acute{\omega}\Delta T) & i_{3r(n)} \\ 0 & 0 & \sin(3\acute{\omega}\Delta T) & \cos(3\acute{\omega}\Delta T) & i_{3i(n)} \end{bmatrix} + \begin{bmatrix} \cos(\acute{\omega}\Delta T) & \sin(\acute{\omega}\Delta T) & 0 & 0 & \Delta i_{r(n)} \\ \sin(\acute{\omega}\Delta T) & \cos(\acute{\omega}\Delta T) & 0 & 0 & \Delta i_{i(n)} \\ 0 & 0 & \cos(3\acute{\omega}\Delta T) & \sin(3\acute{\omega}\Delta T) & \Delta i_{3r(n)} \\ 0 & 0 & \sin(3\acute{\omega}\Delta T) & \cos(3\acute{\omega}\Delta T) & \Delta i_{3i(n)} \end{bmatrix} \tag{3-16}$$

The sampled values obtained from the A to D conversion following DFT are considered as the measurement matrix in the Kalman filter. The measurement matrix will be as follows for both fundamental and harmonic measurements,

$$Z = C \begin{bmatrix} i_{mr(n+1)} \\ i_{mi(n+1)} \end{bmatrix} + noise \tag{3-17}$$

Where, the [C] matrix is the transition matrix of the measurement in to the required form of matrix we require in the future equation. For time being, it is used as a [2x2] diagonal matrix for equation 3-18 and [4x4] diagonal matrix for equation 3-19 as follows.

$$Z = \begin{bmatrix} 1 & 0 \\ 0 & 1 \end{bmatrix} \begin{bmatrix} i_{mr(n+1)} \\ i_{mi(n+1)} \end{bmatrix} + noise \tag{3-18}$$

$$Z = \begin{pmatrix} 1 & 0 & 0 & 0 \\ 0 & 1 & 0 & 0 \\ 0 & 0 & 1 & 0 \\ 0 & 0 & 0 & 1 \end{pmatrix} \begin{matrix} i_{mr(n+1)} \\ i_{i(n+1)} \\ i_{3mr(n+1)} \\ i_{m3i(n+1)} \end{matrix} + noise \tag{3-19}$$

In order to calculate the Kalman gain, it is needed to calculate the process covariance matrix first. Since both $\boldsymbol{i_r}$ and$\boldsymbol{i_i}$are random variables, statistical approach is used in Kalman Filter technique to address the probability and variance of a particular measurement errors. It is assumed that these measurements are distributed as a Gaussian distribution with the expected values (means) and variances (squares of the standard deviations).

Covariance matrix consists of the covariance of two measurement state variables$\mathbf{i_r}$ and$\mathbf{i_i}$ as follows.

$$[P] = \begin{bmatrix} \sigma_r^2 & \sigma_r \sigma_i \\ \sigma_i \sigma_r & \sigma_i^2 \end{bmatrix} \tag{3-20}$$

However, since there is no any relationship between the change or the error or the uncertainty of the state variables $\mathbf{i_r}$ and$\mathbf{i_i}$, we can set the cross terms zero and keep the diagonal values only. The simplified process covariance matrix is as follows.

$$[P]_{n+1} = \begin{bmatrix} \sigma_r^2 & 0 \\ 0 & \sigma_i^2 \end{bmatrix}_{n+1} \tag{3-21}$$

Once the process covariance matrix is determined, Kalman gain can be calculated using following standard form equation.

$$[K] = \frac{[P][C]^T}{[C][P][C]^T + [B]} \tag{3-22}$$

Where

[C] with the same notation as the previous equation 3-18, which allows to convert the process covariance matrix in to the form of Kalman gain matrix. For the matrix which only have the fundamental components,

$$[C] = [1 \quad 1] \tag{3-23}$$

and, matrix with fundamental and third harmonic components,

$$[C] = [1 \quad 1 \quad 1 \quad 1] \tag{3-24}$$

[B] is the is the covariance matrix of the noise inputs of the measurement [Z].

Once the Kalman gain is known, new estimated state values can be obtained using following equation,

$$\begin{bmatrix} i_{rst(n+1)} \\ i_{ist(n+1)} \end{bmatrix} = \begin{bmatrix} i_{rst(n)} \\ i_{ist(n)} \end{bmatrix} + \quad K \ ([Z] \quad [C] \begin{bmatrix} i_{rst(n)} \\ i_{ist(n)} \end{bmatrix} \tag{3-25}$$

$$\begin{bmatrix} i_{rst(n+1)} \\ i_{ist(n+1)} \end{bmatrix} = \begin{bmatrix} i_{rst(n)} \\ i_{ist(n)} \end{bmatrix} + \frac{[P][C]^T}{[C][P][C]^T + [B]} ([Z] \quad [C] \begin{bmatrix} i_{rst(n)} \\ i_{ist(n)} \end{bmatrix} \tag{3-26}$$

In same procedure, new estimated variables for both fundamental and harmonic components also can be obtained.

Before starts the next iteration of the state estimation, it is needed to estimate the new process covariance matrix. From below equation we can obtain the new estimated process covariance matrix.

$$[P]_{n+1} = \begin{bmatrix} P_{11} & P_{12} \\ P_{21} & P_{22} \end{bmatrix}_{n+1} = \begin{bmatrix} 1 & 0 \\ 0 & 1 \end{bmatrix} \quad K\ [C] \begin{bmatrix} P_{11} & P_{12} \\ P_{21} & P_{22} \end{bmatrix}_{n} \tag{3-27}$$

3.2.8. Fault Detection

The difference between the previous estimated value and the measurement can be taken to identify the faults in the network as this value gives the change in the residual current. When all state variables reach a steady-state condition, difference between the previous estimated value and the measurement becomes very small. But if there is any ground fault occurs, this difference become much larger and monitoring this value fault is identified.

If this value is greater than the threshold value we have pre-set, then it moves to the second phase of the algorithm which calculates the third harmonic content of the current waveform. If this value is greater than the threshold value we have set, then HIF is identified.

However, the maximum value of the measurement residual over a cycle is used as a measure of normal measurement residual.

CHAPTER 4

4. SYSTEM MODLING

Information regarding the HIF and its attributes are very much limited due to the practical issues associated with collecting data for practical faults. Lack of information can make it difficult to definitively implement the detection and localization mechanisms while limiting most of the past studies only to the researches. The suggested methodology of this study is simulated using MATLAB SIMULINK which is a block diagram environment for multi domain simulation and model based design.

4.1. HIF Model

An accurate simulation of HIF is essential for the practical development of effective HIF detection algorithms which can implement in real world. The HIF model should reflect it's the complex characteristics of such as asymmetry, nonlinearity, and randomness and dynamic qualities of arcing phenomena.

According to Sedighi [19], HIF models can be divided into 2 groups. First group is based on Emanuel model which was proposed back in 1990 based on the sparks nature when the conductor makes contact with surface. The other HIF models have been categorized as the second group. The simplified Emanuel HIF model in Figure 4.1 is widely used in many HIF simulation experiments, as it combines many of the advantages of previous models and maintains simplicity and accuracy. The parameters of the simplified Emanuel HIF model in Figure 4.1 are shown in Table 4.1 which used in this study.

Table 4.1Parameters of the simplified Emanuel HIF model

Parameter	Value 1	Value 1
R1(Ohm)	200	150
R2(Ohm)	200	150
DC Source 1(kV)	5	4
DC Source 2(kV)	5	4

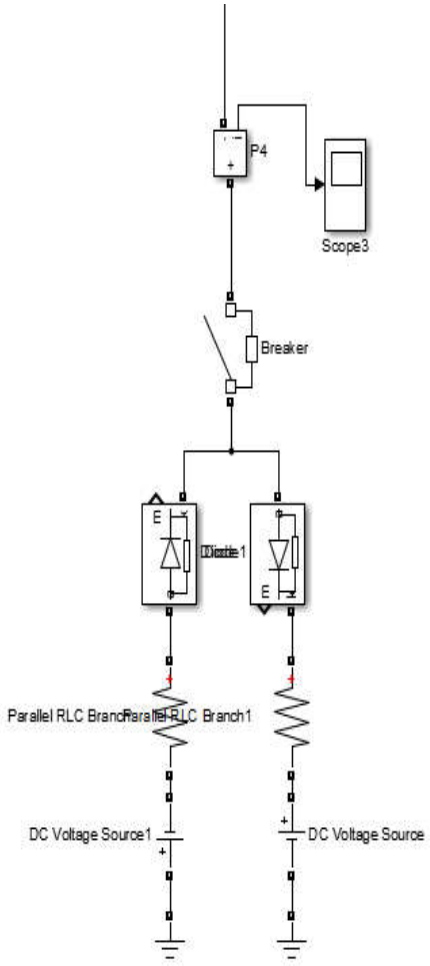

Figure 4.1Simplified Emanuel HIF model

4.2. Modeling of the Distribution Network

Three different distribution networks with different topologies were analyzed with the proposed methodology. All the network topologies were extracted and modeled based on the geospatial network maps of LECO with respective relevant historical load data. Recorded six months average maximum demand of distribution transformers has used as the load data relevant to this section. The transformer loads were categorized as Domestic, Industrial, Commercial or Mixed. Meaning of first three categories has the same meaning of the word, whereas the fourth category was used for transformers feeding a mixture of different types of loads. Industrial loads were considered as constant PQ type and other domestic, commercial and mixed loads were considered as of constant impedance type. Those assumptions are not 100% accurate but as per the traditional load flow analysis methodology; it is assumed that such categorization of the loads will make a balance since it doesn't

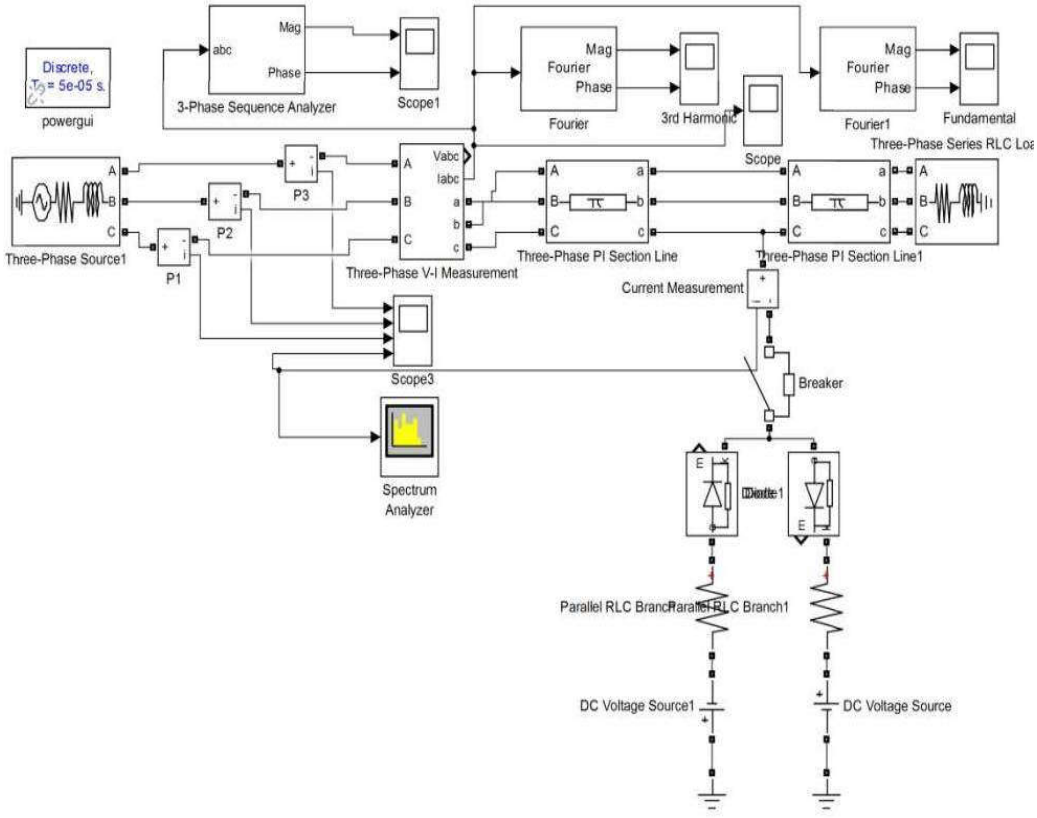

Figure 4.2 HIF Model Used in a Modeled Distribution Network

affect the main focus of this simulation.

All the distribution lines were modeled as actual 150 mm^2 All Aluminium Conductor (AAC) which is commonly named as Hornet. Modeled line parameters are inserted as Figure 4.4.

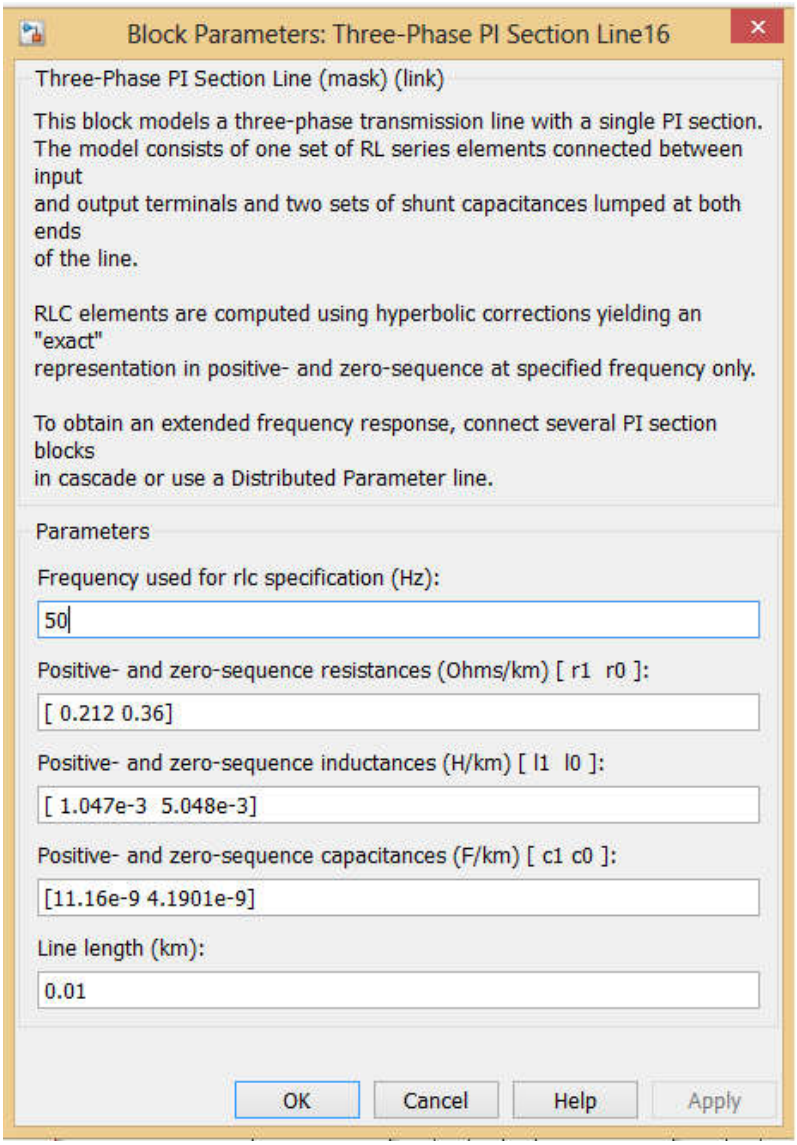

Figure 4.3 Modeled line parameters

Simulated three network topologies are shown in Figure 4.4, Figure 4.5 and Figure 4.6.

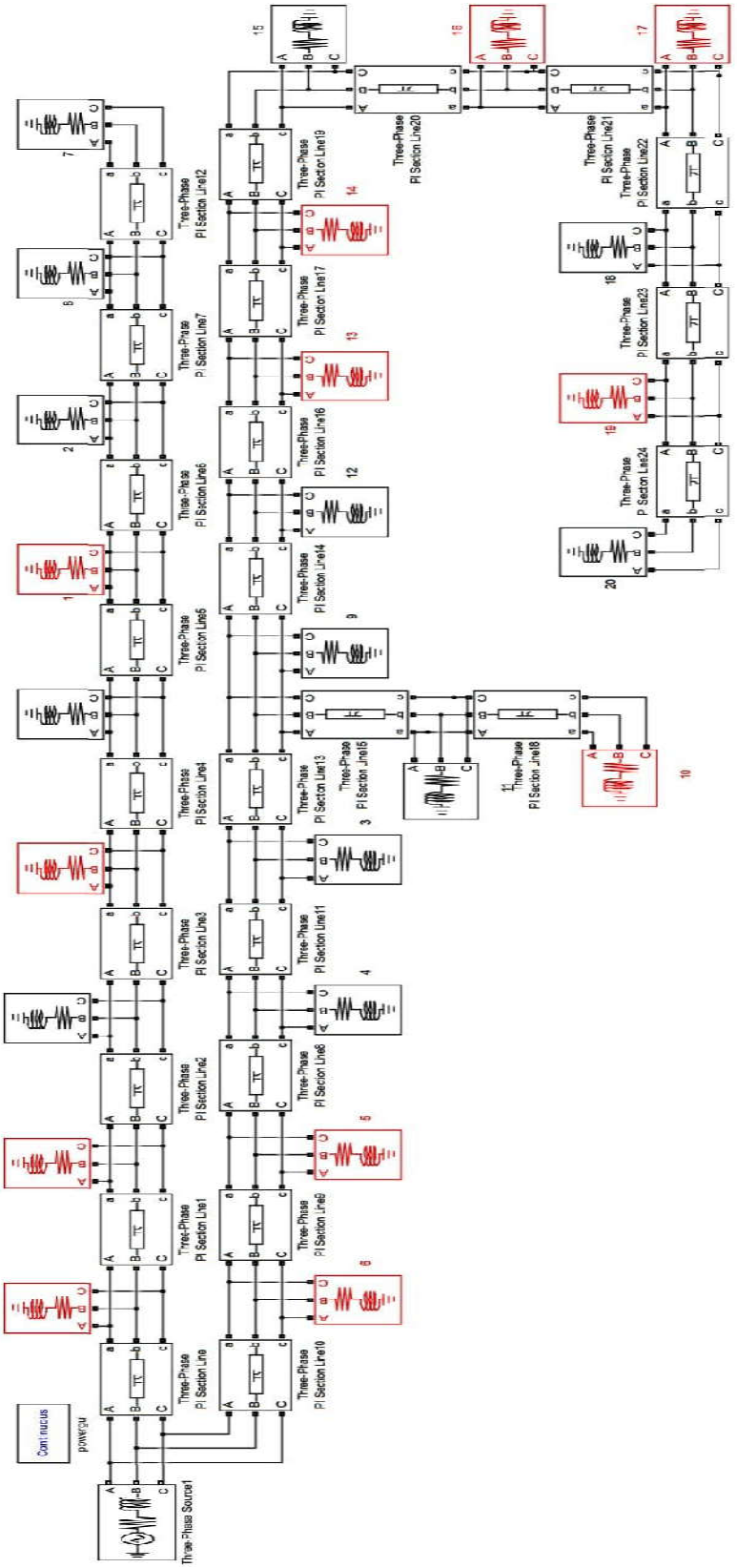

Figure 4.4 Simulated Distribution Network Model 1

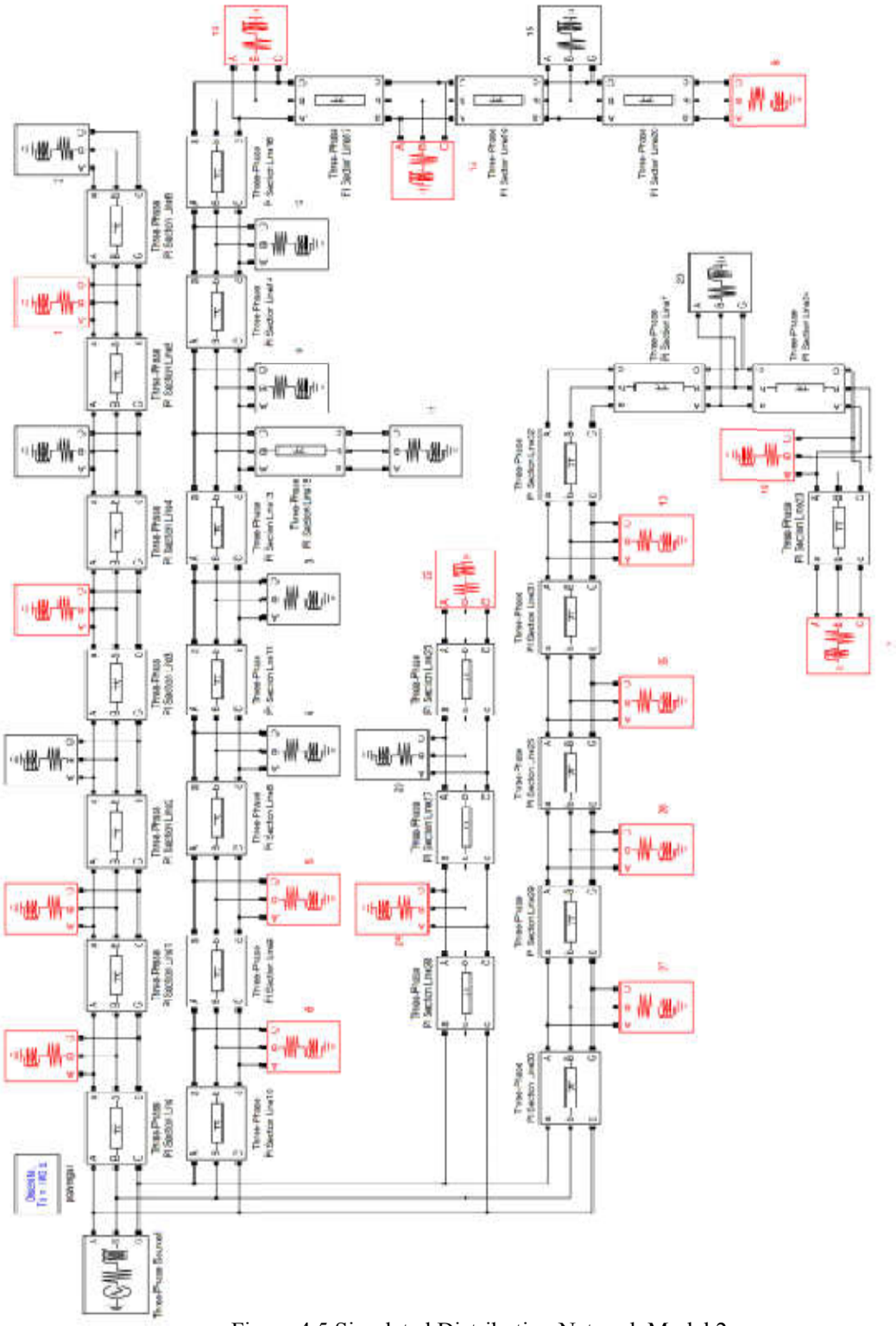

Figure 4.5 Simulated Distribution Network Model 2

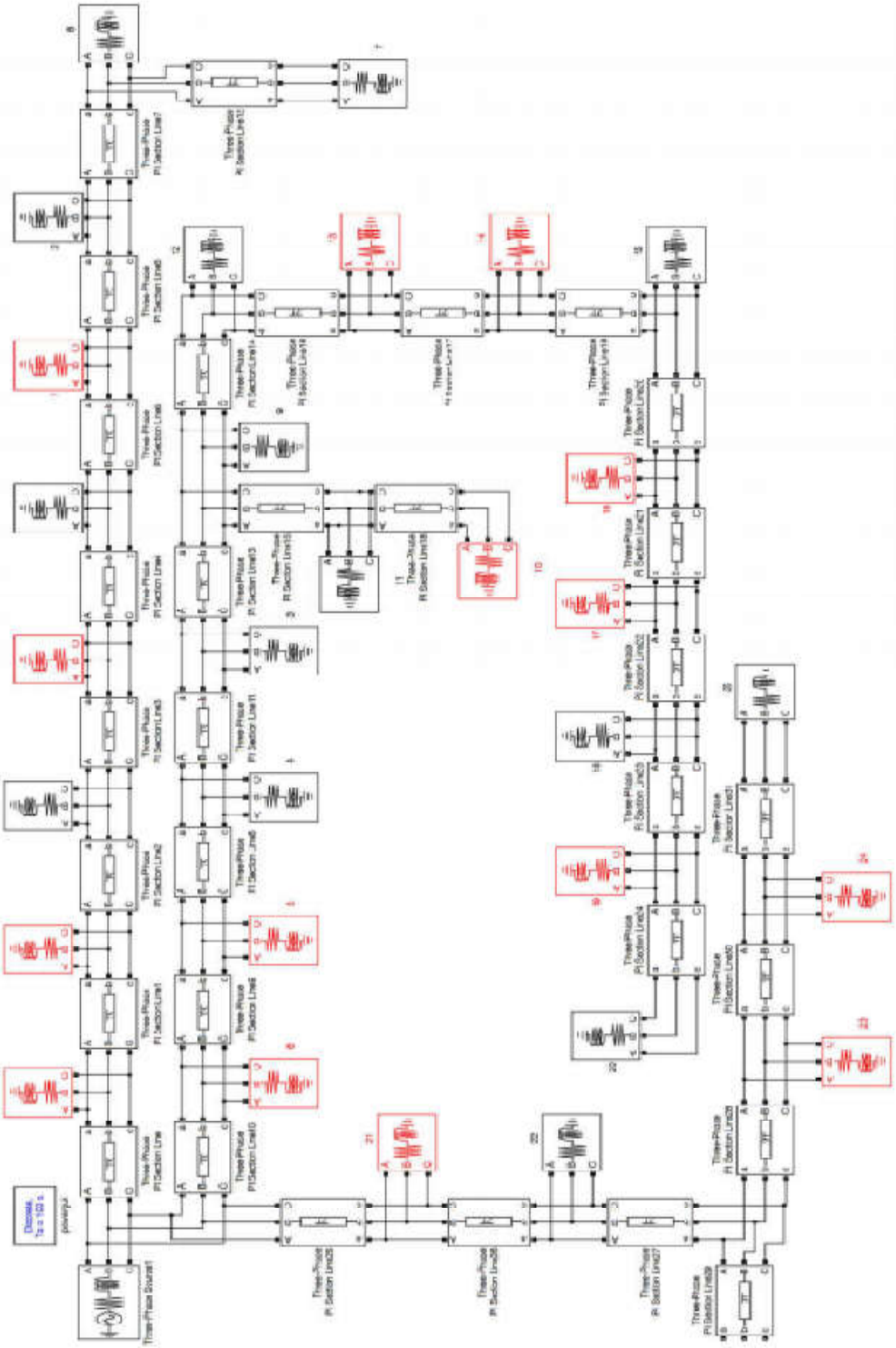

Figure 4.6 Simulated Distribution Network Model 3

4.3. Design of a Kalman Filter

The Kalman Filter is a non-linear time domain estimator which used in this study to identify HIF by estimating the current waveform and the harmonic components of it. Practical current waveforms are comprised with various ripples and noises where Kalman Filter can minimize these errors with its recursive estimation methodology to obtain the estimated fundamental and harmonic components.

In this study, it is suggested to have two states for the algorithm which referred as steady state and the alert state for the Kalman Filter implementation.

4.3.1. Steady State Kalman Filter Implementation

In the steady state, a Kalman filter is implemented for a period of 1 cycle current waveform which the ΔT=20 ms. Then, the state transition matrix as for the equation 4.1 is as follows.

$$[A] = [B] = \begin{bmatrix} \cos(2\pi) & \sin(2\pi) \\ \sin(2\pi) & \cos(2\pi) \end{bmatrix} \tag{4-1}$$

$$[A] = [B] = \begin{bmatrix} 1 & 0 \\ 0 & 1 \end{bmatrix} \tag{4-2}$$

Then the state transition matrix becomes,

$$\begin{bmatrix} i_{r(n+1)} \\ i_{i(n+1)} \end{bmatrix} = \begin{bmatrix} 1 & 0 \\ 0 & 1 \end{bmatrix} \begin{bmatrix} i_{r(n)} \\ i_{i(n)} \end{bmatrix} + \begin{bmatrix} 1 & 0 \\ 0 & 1 \end{bmatrix} \begin{bmatrix} \Delta i_r \\ \Delta i_i \end{bmatrix} \tag{4-3}$$

The measurement matrix for the current waveform in steady state is as follows.

$$Z = \begin{bmatrix} 1 & 0 \\ 0 & 1 \end{bmatrix} \begin{bmatrix} i_{mr(n+1)} \\ i_{mi(n+1)} \end{bmatrix} + noise \tag{4-4}$$

For the convenience of this study, it is assumed that noise portion of the measurement matrix is zero as we are getting inputs from a simulation. In real practical application, it is necessary need to consider the noise component as a white

Gaussian noise in order to obtain an optimum Kalman Filter design. Therefore, measurement matrix is as follows.

$$Z = \begin{bmatrix} 1 & 0 \\ 0 & 1 \end{bmatrix} \begin{bmatrix} i_{mr(n+1)} \\ i_{mi(n+1)} \end{bmatrix} \tag{4-5}$$

In this study, the current phasor with real component and an imaginary component varies randomly from one sampling interval to the other due to load changes in the distribution network. The standard deviation of the current changes assumed to be 0.004 per unit from an empirical study did to find the best coefficient which takes the system in to stable in minimum amount of time.

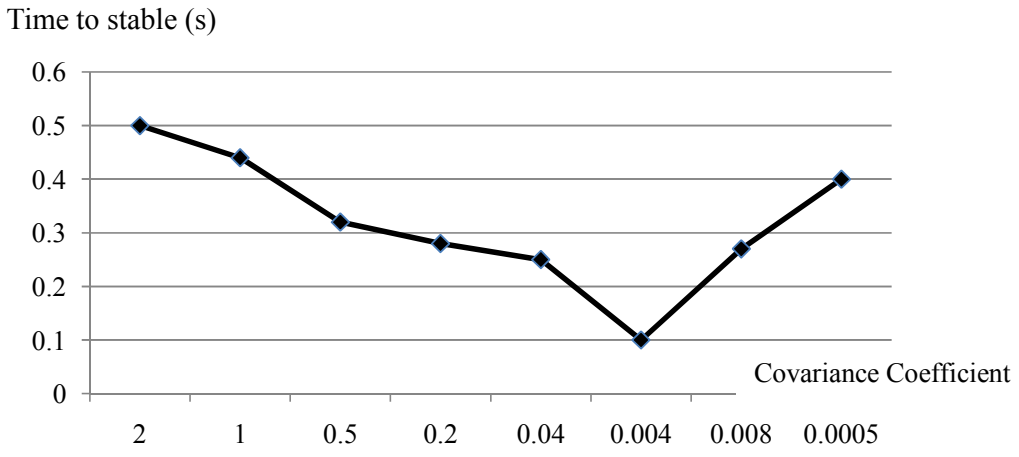

Figure 4.7 Time for Stalbe with Different Covariance Coefficients

Further, in real world scenario, these load variations with high frequency sampling, considerable amount of measurement errors are experienced. But since this is a simulation, it is assumed that there are no any measurement errors and standard deviation of these measurement errors are zero.

Therefore, the initial process covariance matrix as per the equation 4.6 is as follows.

$$[P] = \begin{bmatrix} 0.004^2 & 0 \\ 0 & 0.004^2 \end{bmatrix} \tag{4-6}$$

By using above process covariance matrix, Kalman gain can be found and estimated state can be calculated once cycle at a time. Before calculating the recursive next estimation, difference of the measured value and the previous estimated value is calculated.

$$MG = \frac{[Z] \quad [C] \begin{bmatrix} i_{rst(n)} \\ i_{ist(n)} \end{bmatrix}}{[C] \begin{bmatrix} i_{rst(n)} \\ i_{ist(n)} \end{bmatrix}} \tag{4-7}$$

This value can be varies over the time due to the data sampling errors and nonlinearity occur in the A to D conversion of the conductor mounted devices with the aging. Therefore, residual signal of equation 4-7 can identify a magnitude which depends on the accuracy and the time linearity of the device. However, it is assumed that this effect of this non linearity does not make the equation 4-7 greater than two.

If the measurement value is greater than two times the previous estimated value, then there is a possibility of a low impedance fault or a HIF. If the system detects such a value for the equation 4-7, system moves to the alert state estimation where system seeks for possible third harmonics in the residual current.

4.3.2. Alert State Kalman Filter Implementation

If the system moves in to the Alter State, system calculates the third harmonic levels of the waveform to detect HIFs. Further, the ΔT used which is 20 ms also get reduced to the sampling frequency which is 0.667 ms (1.5kHz).The fundamental phasor variation due to this time interval can be considered as 12^0 . Therefore, in order to estimate the third harmonic content of the waveform, state transition matrix changes in to the form of equation 4-9.

$$[A] = [B] = \begin{bmatrix} \cos(12) & \sin(12) & 0 & 0 \\ \sin(12) & \cos(12) & 0 & 0 \\ 0 & 0 & \cos(36) & \sin(36) \\ 0 & 0 & \sin(36) & \cos(36) \end{bmatrix} \tag{4-8}$$

$$[A] = [B] = \begin{bmatrix} 0.978 & 0.207 & 0 & 0 \\ 0.207 & 0.978 & 0 & 0 \\ 0 & 0 & 0.809 & 0.587 \\ 0 & 0 & 0.587 & 0.809 \end{bmatrix} \quad (4\text{-}9)$$

By using this state transition matrix and the relevant following up equations, we can estimate the third harmonic level of the current waveform. By allowing a withstanding range to measurement and sampling errors, if the third harmonic content of the particular waveform prolongs greater than 30% up to four cycles it is concluded that this particular RTU has identified a HIF.

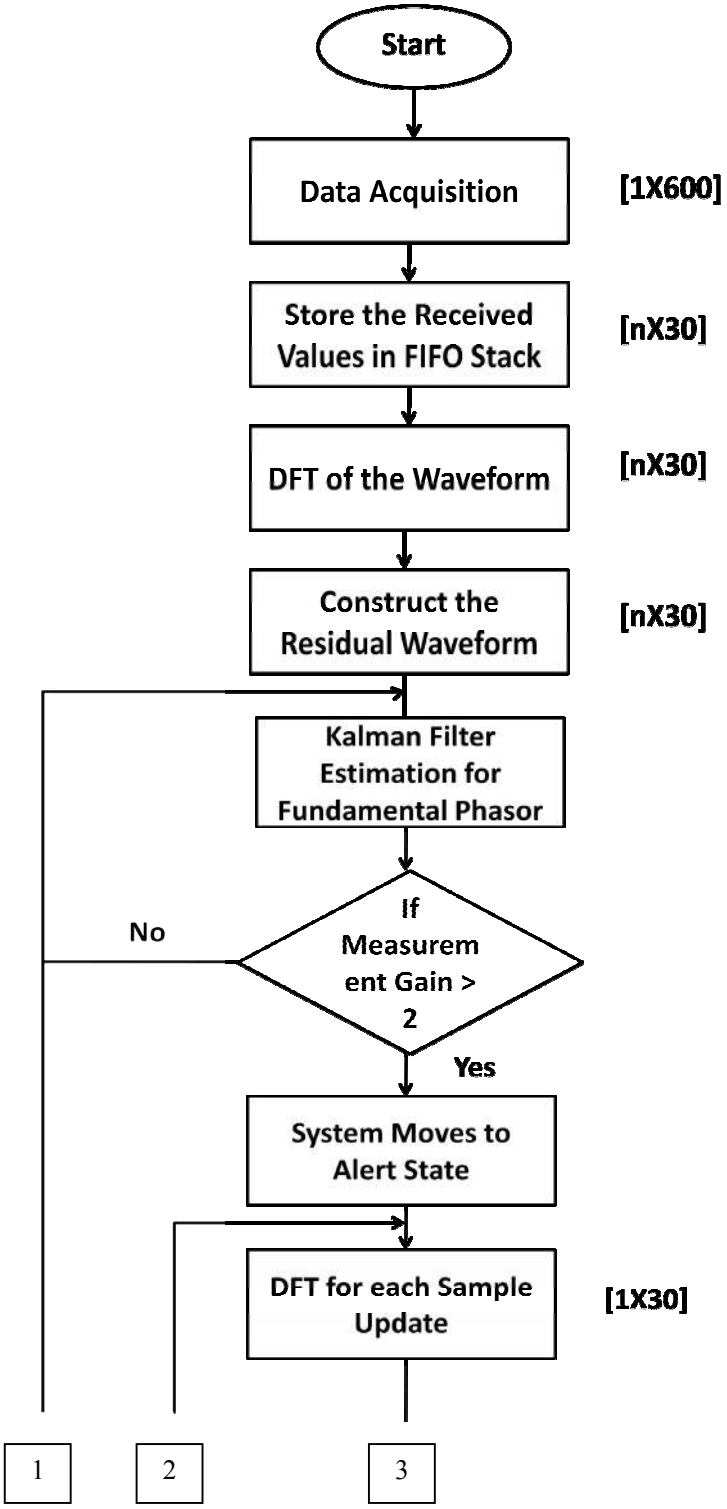
Start
Data Acquisition
[1X600]
Store the Received Values in FIFO Stack
[nX30]
DFT of the Waveform
[nX30]
Construct the Residual Waveform
[nX30]
Kalman Filter Estimation for Fundamental Phasor
If Measurement Gain > 2
No
Yes
System Moves to Alert State
DFT for each Sample Update
[1X30]
1
2
3

Continued from previous page,

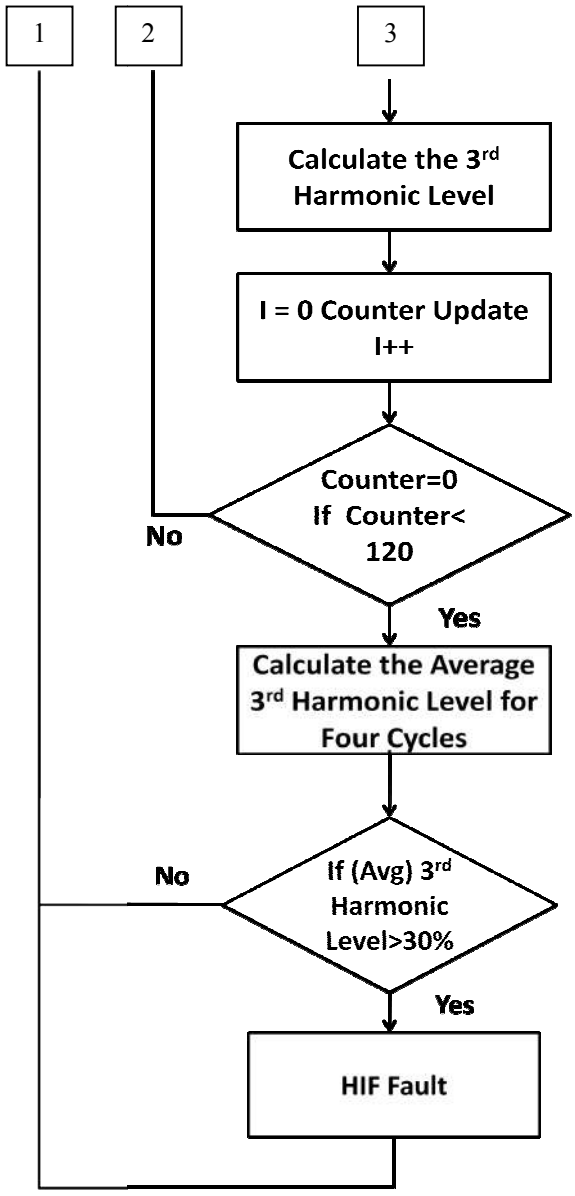

Figure 4.8 Proposed Algorithm

4.3.3. Simulations

Three different 11kV distribution networks are simulated using MATLAB/SIMULINK environment implementing the proposed HIF detection methodology. The results are described in Chapter 5.

CHAPTER 5

5. RESULTS

The validated Emmanuel HIF model and the modeled real 11kV distribution networks with the HIF detection algorithm wasimplemented in the MATLAB/SIMULINK environment and analyzed for following different four network case scenarios.

1. Case I - High load variationsof single phase loads
2. Case II - High load variationsof three phase loads - (15 times for three different networks with before and after HIF location along the feeder)
3. Case III - Capacitor bank switching (both connecting and disconnecting15 times for three different networks with before and after HIF location along the feeder)
4. Case IV - Low impedance fault - (15 times for three different networks with before and after HIF location along the feeder)

5.1. Case I - High load variationsof single phase load

Load variations play a significant impact during identification of HIFs during the faulty and non-faulty conditions. Since the current variation during the HIF is also in the same scale as per the current variation in the normal operation, it is hard to detect and differentiate low current HIFs from normal operation using conventional fault detection methods. Therefore this study analyzed 15 times of HIFs with single phase load which varies at a high rate during its normal operation. This creates a temporary unbalance situation in the network and HIF occurs within this network turbulence was analyzed. Further HIF location is also significant in identifying the HIF as the current drawn for the fault is highly varying with the fault location. Therefore this combination covers high load variation spot loads located both before and after the HIF as per the sample figure 5.1.

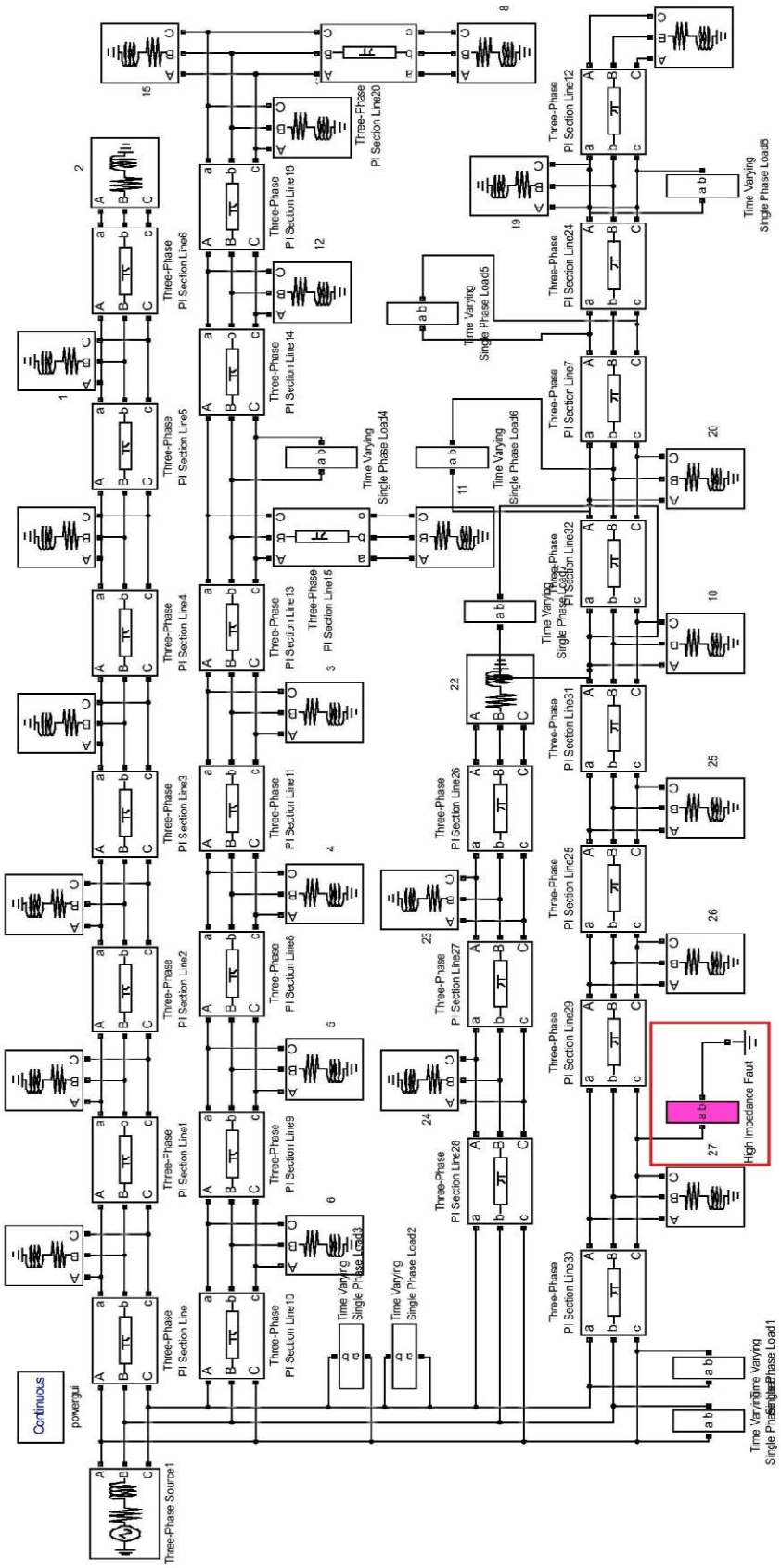

Figure 5.1 HIF with Highly Varying Single Phase Loads

5.2. Case II - High load variationsof three phase load

Three phase loads also play a significant impact during HIF identification when it is running on unbalance conditions. This effect could be much critical when these unbalances are varying with the time as a random function. Therefore this study analyzed 15 times of HIFs with unbalance three phase loads which varyin arandom nature with high load variation to make the network an unexpectedly volatile with HIF is located different locations along the network. One of such sample network is illustrated in figure 5.2.

5.3. Case III – Capacitor Bank Switching

Capacitor switching occasions like disconnecting and re-connecting individual capacitors as well as banks also make significant impacts in HIF identification as theses occasions creates same non linearity like HIF. Most often these capacitor bank switching creates high percentages of harmonics for a shorter period which are not sustaining for longer duration like HIF Capacitor disconnection increases the load from small amount with significant harmonic content which almost same as the HIF. Capacitor re-connection also generates certain amount of harmonics but if this combined with another linear or non linear load increasing occasion, this can be seen same as a HIF. Figure 5.3 illustrates a sample network diagram of such a simulation and figure 5.7 illustrates the 3^{rd} harmonic estimation of the algorithm with a capacitor bank switching simulated in parallel with the HIF.

5.4. Case IV - Low Impedance Fault

Low impedance single phase to ground faults are much frequent in distribution networks. This type of faults are associated with significant amount of zero sequence current components which triggers the circuit breakers to trip instantaneously or with particular time duration depending on the magnitude of the fault current, protection settings and sensitivity of the system. Therefore, these faults are detected and cleared immediately with conventional protection mechanisms. This study tried to identify the accuracy of the algorithm of identifying HIF during a low impedance fault appeared in the network simultaneously. Figure 5.4 illustrates a sample network

diagram of such a simulation and figure 5.8 illustrates the residual and phase currents resulted due to that fault.

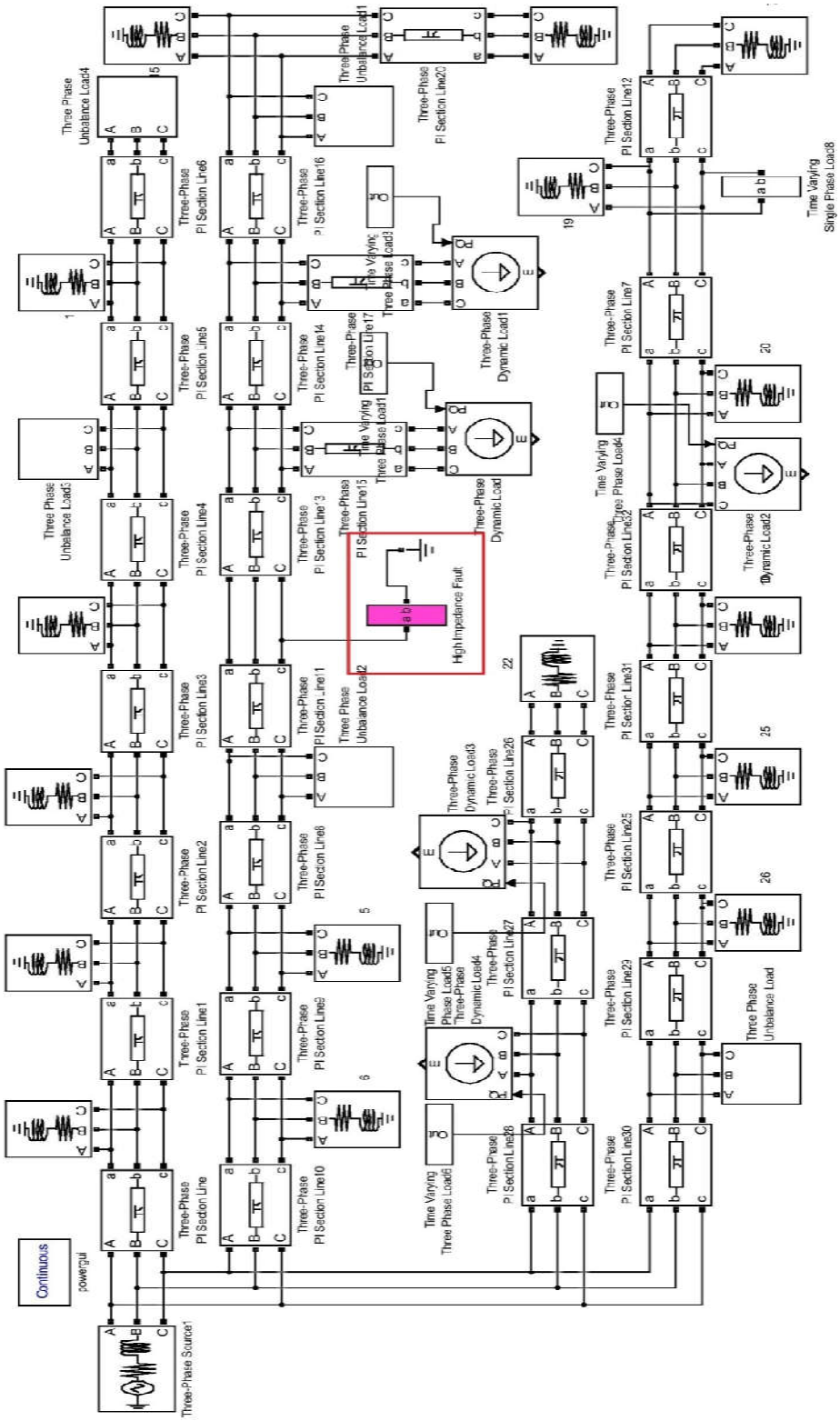

Figure 5.2 HIF with Highly Varying Three Phase Unbalance Loads

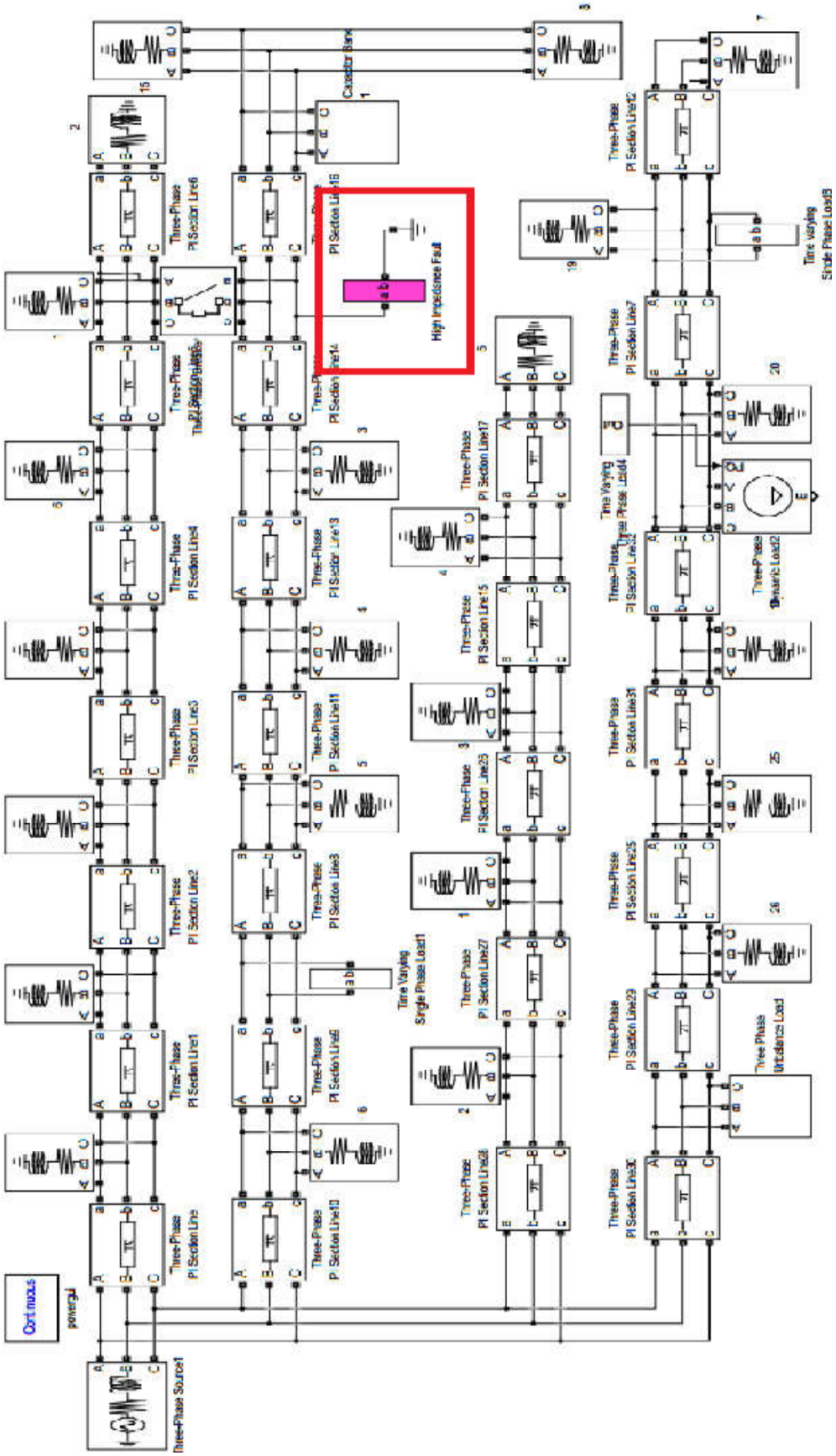

Figure 5.3 HIF with Capacitor bank switching

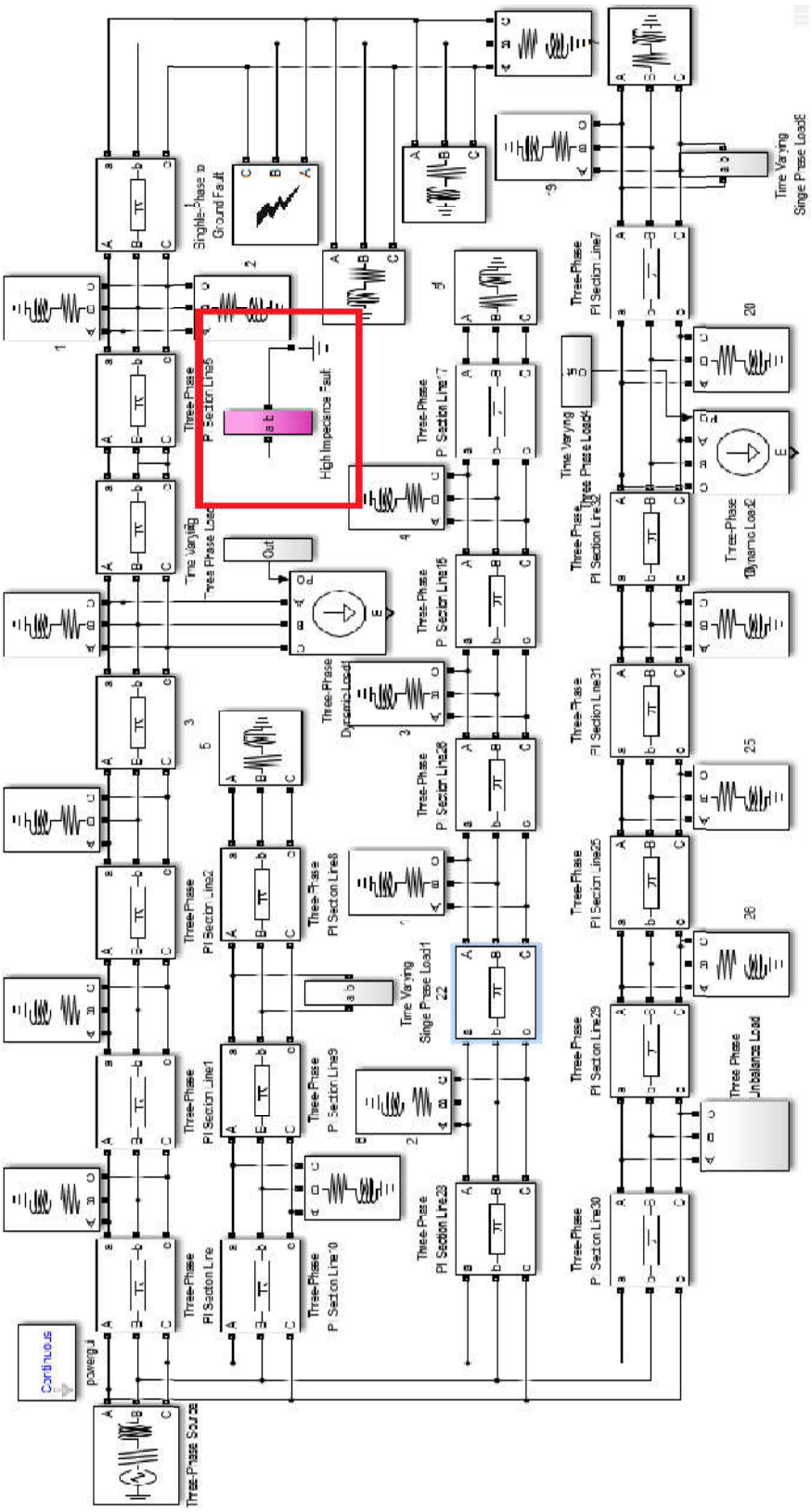

Figure 5.4HIF with Low Impedance Fault

From above different network fault cases and conditions, mutually, 128different cases were simulatedwith the fault detection algorithm. Figure 5.5 shows the simulated phase currents and residual current when a HIF occurred within 0.15s to 0.25s. It clearly illustrates the problem statement of the HIF detection where only the residual identifies the HIF while other phase currents does not show any significant load change during the fault.

The estimated 3rd harmonic for this particular fault is shown in figure 5.6. Initially recursive estimation optimizes its variables and stabilized in the steady state region and identifies the fault from sustained third harmonic content starting from time it originates. Since all these are noise free measurements taken from the simulation, the results are more accurate and fast responsive. Table 5.1 shows the results obtained for the 128combinations of simulations.

Table 5.1 Simulation Results

Description	**Actual HIF**	**Non Faults**
Detected HIF	106	0
Not detected	15	7

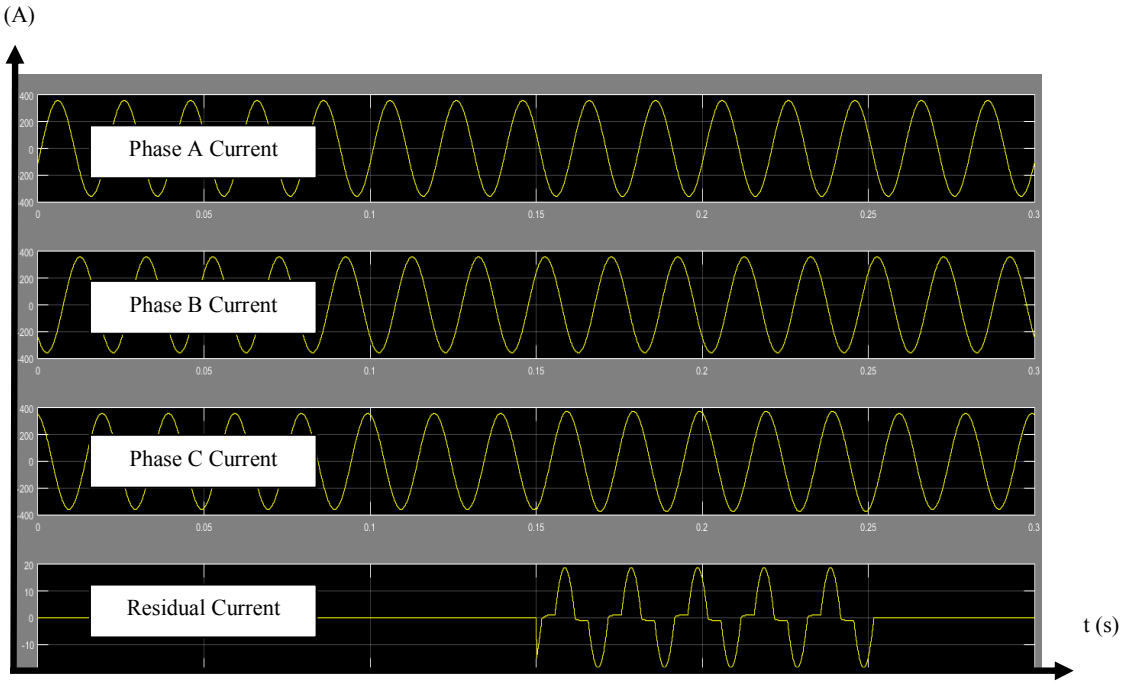

Figure 5.5 Simulated Phase Current and Residual Current

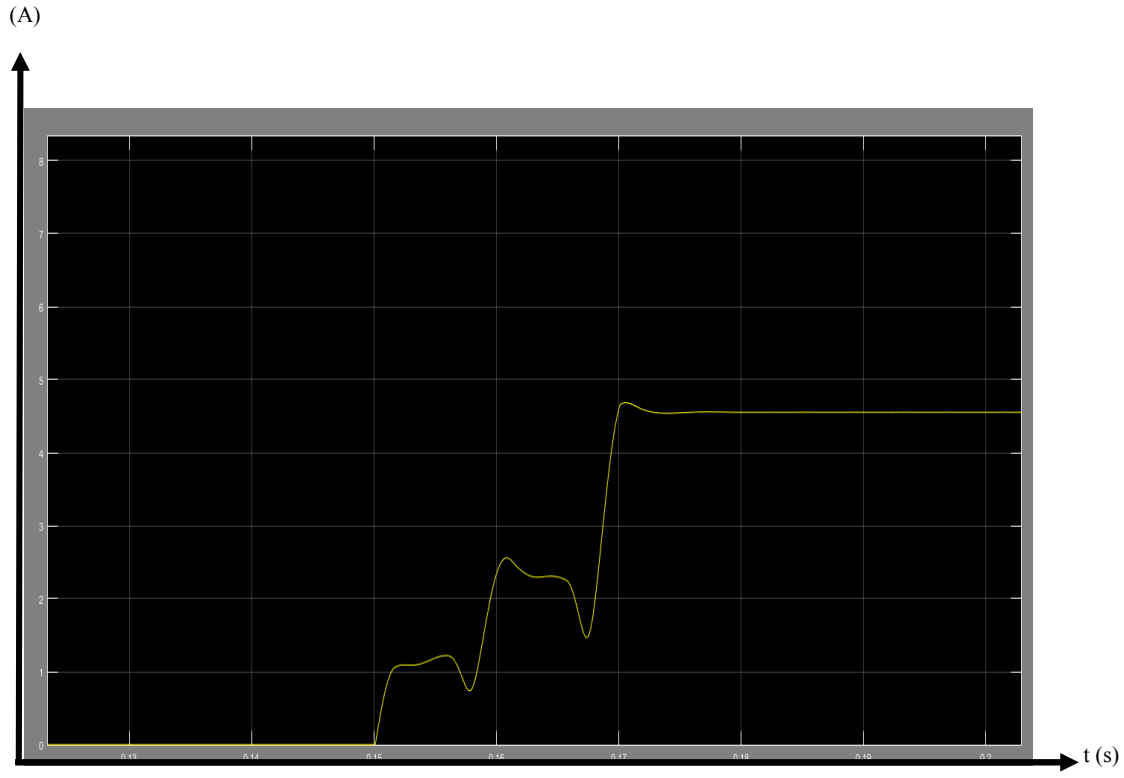

Figure 5.6 Estimated 3rd Harmonic Current Magnitude for Case 1 Type Fault

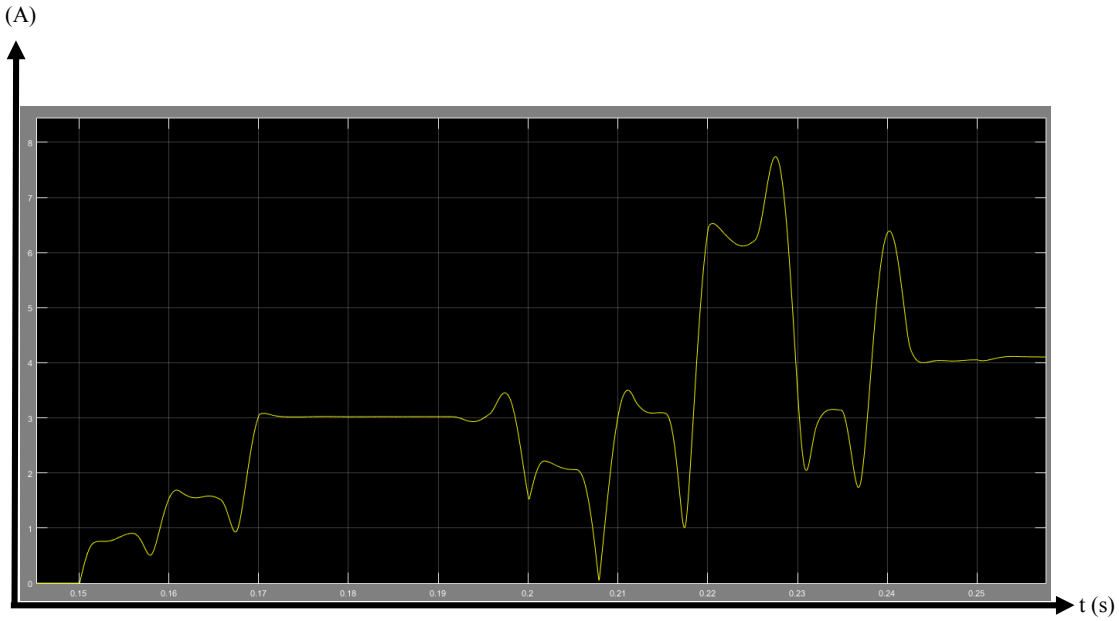

Figure 5.7 Estimated 3rd Harmonic Current Magnitude for Case 3 Type Fault

It is observed that 87.06% of the HIF were identified by the proposed methodology and only 12.94% of HIF were unable to detect. Further, it is observed that all these 15 cases were the low impedance fault cases where significant amount of residual currents were appeared during the fault.

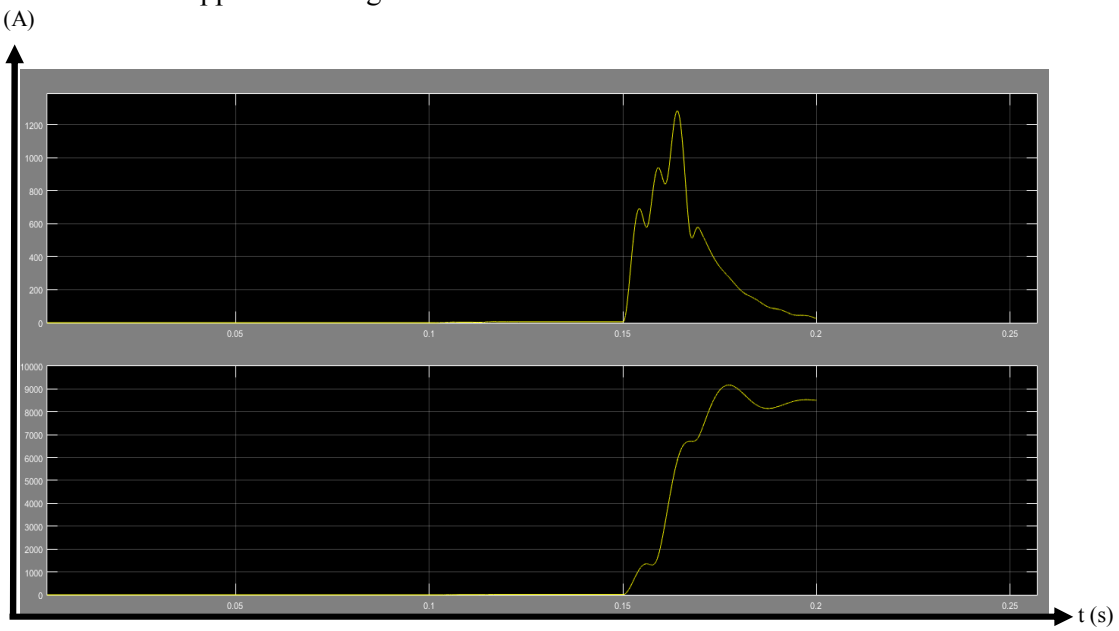

Figure 5.8 Residual current and phase Current of low impedance fault

It is observed that accuracy of detecting a fault is high as 87% while accuracy of not detecting a non fault is 100% as per the all simulated cases.

Further, in order to analyze the fault sensitivity of the proposed system, a response time test was done against different fault impedances for case 1 type fault and Figure 5.9 depicts the results of this test.

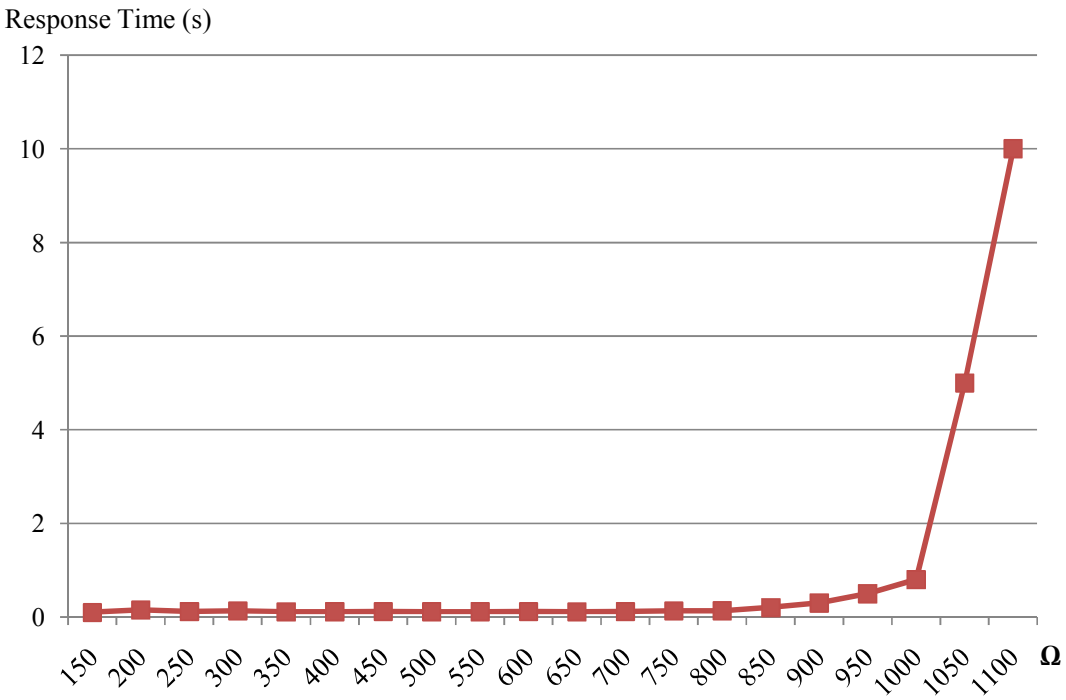

Figure 5.9 Response Time of System for Different Fault Impedances

It is observed that this algorithm could detect high impedance faults up to 1000 ohms within 150ms and if the impedance is further increased, it takes longer time to response. This is mainly due to the limited fault current draws during these faults. Generally if 11 kV network considered, LECO uses 500 ohms ground fault path impedance from the 6km away the primary substation as the current setting for the primary substation relay. This gives 12.7A residual current which trigger the circuit breaker in 3 seconds if IEC standard inverse curve is considered.

CHAPTER 6

6. Conclusion

Earth faults occurring in electrical distribution systems are categorized in to two categories depending on the fault impedance namely Low Impedance Faults and High Impedance Faults. Overhead bare distribution systems likes the 11 kV network of Lanka Electricity Company (Private) Limited, are more prone to physical contact or arc with nearby objects which are mostly not very conductive. Most of the time these situations can create above said high impedance faults which are very difficult to differentiate and locate in midst of normal operational load conditions. This is mainly due to the limited current it draws which is not enough to operate the conventional over current protection mechanisms, such as fuses and over current relays, if the instruments are not specifically designed. This small fault current, or the very small increment, in the feeders appears to be a normal load increment during the operation. Most of the times, these HIFs creates arc flashes as a result of the air gap breakdown between the conductor and a quasi-insulated object or the earth surface. This increases the hazardousness of these types of faults as it can be prone to initiate a fire if not cleared immediately. Further HIFs creates an immense burden on system operators and field staff on locating due to the limited fault visibility. Field staff repetitively switches on and off the load breaker switches to isolate sections to find the exact location of the fault to repair and restore the supply.

This studyhas successfully implemented a new HIF detection algorithm based on estimating the residual load variation and 3^{rd}harmonic content and increment of the residual currents,in MV distribution network using a Kalman Filter. This developed methodology that can be simply implemented by the utilities to identify and localize the HIF with proposed hardware architecture.

This study has proposed a unique, low cost time stamp based data acquisition device which can be hanged on conductors to collect the required data and transmit through a wireless network to a remote terminal unit (RTU) mounted on the pole. Three pre-calibrated conductor mounted analog to digital high frequency data converters

acquires the three current waveforms data with a time stamp synchronized with the internal clock to the UTC with assist of a GPS receiver. These three phasor data are transmitted to a pole mounted RTU which act as the data concentrator andanalyses the waveforms and residuals to notify a central server about the identified network anomaly.

Due to the high volatility of the field current measurements of the distribution network, a Kalman Filter based approach has been used in this research to analyze the residual current of the three phases. This analysis is done by the pole top RTU which basically combines all three current waveforms and estimates the residual current waveform. Using a Kalman filter gives the additional advantage to get rid of the noise associated with the raw signals and digital signal processing.

A state space model is developed for the residual waveform estimation in order to implement the Kalman filter technique. Avalidated Emanuel HIF model is used for the simulations of the HIFs to test the developed algorithm. Simulations were carried out by modeling three real 11kV distribution networks using MATAB/SIMULINK environment by creating four different cases namely HIFs with high load variations of single phase load, high load variations of three phase load, capacitor bank switching and low impedance fault. These were analyzed for possible HIF faults with combination of different network scenarios for totally 128 simulation combinations. It is observed that accuracy of detecting a fault is high as 87% while accuracy of not detecting a non fault is 100% Further it is identified that due to the high zero sequence current component in during the low impedance fault, the properties of HIF are overshadowed and this algorithm couldn't detect the fault accurately. It was concluded that probability of occurring HIF simultaneously with a low impedance fault is very low and in such scenario, network will be tripped due to the low impedance fault. Therefore, hazardous situation of HIF can be mitigated temporary.

This study has limitations like not consideration of noise data, off nominal frequencies and 1 PPS pulse error in different devices and communication delays of the network which need to be addressed during the practical implementation.

References

1. Suresh Gautam; Sukumar M. Brahma, "Detection of High Impedance Fault in Power Distribution Systems Using Mathematical Morphology," IEEE Transactions on Power Systems, vol. 28, no. 2, pp. 1226-1234, May 2013.
2. High Impedance Fault Detection Technology, Report of PSRC Working Group D15 March 1, 1996
3. A. V. Masa, J.-C. Maun and S. Werben, "Characterization of high impedance faults in solidly grounded distribution networks," in 17th Power Systems Computation Conference (PSCC), Stockholm, Sweden, 2011.
4. HRL Technology Pvt. Ltd, "Probability of Bushfire Ignition from Electric Arc Faults", Report HLC/2010/95,2011
5. Modelling and detection of high impedance faults Huwei Wu; B. T. Phung; Daming Zhang; Jichao Chen, 2014 International Conference on Smart Green Technology in Electrical and Information Systems (ICSGTEIS)
6. K. Nara, J. Hasegawa, T. Oyama, K. Tsuji, T. Ise, "FRIENDS – Forwarding to Future Power Delivery System," Conf. Record of IX IEEE International Conference on Harmonics and Quality of Power, Orlando October 2000, pp. 8-18.
7. Mora-Flòrez J, Meléndez J, Carrillo-Caicedo G. Comparison of impedance based fault location methods for power distribution systems. Electr Power Syst Res 2008;78:657–66.
8. C. Orozco-Henao, A.S. Bretas, R. Chouhy-Leborgne, A.R. Herrera-Orozco, J. Marín-Quintero, Active distribution network fault location methodology: A minimum fault reactance and Fibonacci search approach Electrical Power and Energy Systems 84 (2017) 232–241
9. M. Mirzaei, M.Z. A Ab Kadir, E. Moazami, H. Hizam, Review of Fault Location Methods for Distribution Power System Australian Journal of Basic and Applied Sciences, 3(3): 2670-2676, 2009.
10. Martins, L.S., J.F. M a rtins, C.M. Alegria and V.F. Pires, 2003. A Network Distribution Power System Fault Location Based on Neural Eigenvalue Algorithm. In Proceeding of IEEE Bologna PowerTech Confere nce, Bologna, Italy.
11. W ang, C.,H. Nouri and T.S. Davies, 2000. A Mathematical Approach for Identification of Fault Sections on the Radial Distribution Systems, 10th Mediterranean Electro technical Conference (MELECON), 3: 882-886.

12. Carl L. Benner, Member, IEEE, and B. Don Russell, Fellow, IEEE, Practical High-Impedance Fault Detection on Distribution Feeders, IEEE TRANSACTIONS ON INDUSTRY APPLICATIONS, VOL. 33, NO. 3, MAY/JUNE 1997.
13. Macedo, J.R., Resende, J.W., Bissochi, C.A., et al.: 'Proposition of an interharmonic-based methodology for high-impedance fault detection in distribution systems', IET Gener. Transm. Distrib., 2015, 9, (16), pp. 2593–2601
14. Jichao Chen, Toan Phung, Trevor Blackburn, Eliathamby Ambikairajah, Daming Zhang, Detection of high impedance faults using current transformers for sensing and identificationbased on features extracted using wavelet transform, IET Gener. Transm. Distrib., 2016,9,(10), p. 2990 – 2998
15. Mohd Syukri Ali1, Ab Halim Abu Bakar, Hazlie Mokhlis, Hamzah Aroff, Hazlee Azil Illias, Muhammad Mohsin Aman, High Impedance Fault Localization in a Distribution Network using the Discrete Wavelet Transform, 2012 IEEE International Power Engineering and Optimization Conference (PEOCO2012), Melaka, Malaysia.
16. Ali-Reza Sedighi, Mahmood-Reza Haghifam, O. P. Malik, Mohammad-Hassan Ghassemian, High Impedance Fault Detection Based on WaveletTransform and Statistical Pattern Recognition, IEEE Transactions On Power Delivery, VOL. 20, NO. 4, OCTOBER 2005.
17. S. R. Nam, J. K. Park, Y. C. Kang, T. H. Kim, "A Modeling Method of a High Impedance Fault in a Distribution System Using Two Series Time-Varying Resistances in EMTP", IEEE,Vol. 2, pp.1175-1180,2001.
18. Naser Zamanan, Jan K. Sykulski, "Modeling arcing high impedances faults in relation to the physical processes in the electric arc" WSEAS Transactions On Power Systems, Issue 8, Volume 1, August 2006.
19. A. R. Sedighi and M. R. Haghifam, "Simulation of High Impedance Ground Fault In Electrical Power Distribution Systems," in Power System Technology (POWERCON), Hangzhou, 2010.